

Review

# Recycling in Building Materials: Analysis of the Possibilities and Results of Using Recycled Glass Sand in Autoclaved Materials

Anna Stepien 

Civil Engineering and Architecture, Kielce University of Technology, Al. 1000-lecia P.P. 7, 25-314 Kielce, Poland; ana\_stepien@wp.pl

**Abstract:** The construction industry is particularly responsible for the appearance of the earth and the environment and for its partial degradation related to climate warming through the production of cement, brick burning, and the processing of substrates for the production of building materials (lime, gypsum, polystyrene, processed materials, etc.). An important aspect of the 21st century has been the overproduction and excessive use of natural resources, including sand. The purpose of this article is to analyze the possibility of using glass sand as a substitute for quartz sand in the production of materials resulting from hydrothermal treatment (so-called silicate bricks). The article is a review of the research conducted since 2016 on laboratory tests on the modification of silicate mass with glass sand from recycled bottle glass, the properties of the mass modified in this way (hydration temperature, consistency, and humidity of the mixture), its physical and mechanical properties, and its structural and potential durability, which is related to, e.g., the direction and degree of crystallization of the C-S-H phase. Tests of compressive strength, density, water absorption, oxide composition (XRF), structure (XRD), microstructure (SEM), and porosity (CT analysis using computer tomography) were carried out. A special point of the research was the use of geochemical modeling code in the form of the GEMS-PSI program in the process of analyzing the modification of silicate mass by glass sand, which is beneficial in limiting ineffective modifications, thus saving time, money, and energy. Studies have shown that the use of glass cullet has a positive effect on the consistency of the modified raw material mass, on the density ( $1.6\text{--}1.75\text{ kg/dm}^3$ ), and on the compressive strength (15.729–20.3 MPa), while the crystallization of the C-S-H phase occurs in the direction of natrolite and gyrolite, less frequently towards the M-S-H or brucite phase.



**Citation:** Stepien, A. Recycling in Building Materials: Analysis of the Possibilities and Results of Using Recycled Glass Sand in Autoclaved Materials. *Energies* **2023**, *16*, 3529. <https://doi.org/10.3390/en16083529>

Academic Editor: F. Pacheco Torgal

Received: 14 February 2023

Revised: 11 March 2023

Accepted: 7 April 2023

Published: 19 April 2023



**Copyright:** © 2023 by the author. Licensee MDPI, Basel, Switzerland. This article is an open access article distributed under the terms and conditions of the Creative Commons Attribution (CC BY) license (<https://creativecommons.org/licenses/by/4.0/>).

## 1. Introduction

Stone, wood, bricks, and concrete are materials that have been commonly used for years in everyday construction. The rapid urbanization of our world is a resource-intensive process that has led to an irreversible, unsustainable transfer of material from nature to anthropogenic resources [1,2]. The 20th century saw a rapid increase in the stock of materials stored in buildings. Unfortunately, this means the constant destruction of trees for wood, extraction of natural resources for cement and sand, and gravel for concrete and bricks. Natural aggregates account for approximately 1/3 of the raw materials and materials used in the world, and in terms of quantity, they are the largest group of extracted minerals. The global production of aggregates is estimated at over 20 billion Mg/year, although precise data are not available. Gravel-sand and broken aggregates are used mainly in the construction industry for the production of concrete, roads, or as substrates for the production of, among others: asphalt, mortar, and adhesives, prefabricated products, macroleveling, sports infrastructure, mining backfills, etc. [3–5]. Therefore, in the 21st century, the possibility of relieving the natural sources of building materials constitutes

the basis of construction and attempts to introduce components, e.g., from recycling. However, it should be remembered that the outer wall should be a safe barrier against the environment—protect from frost, wind, fire, or noise. Simultaneous fulfillment of these requirements at an appropriate level is possible by using the so-called function wall or by targeted modification of building materials because, masonry walls were and still are the main structural element of buildings, which naturally should be resistant to lateral forces and changes occurring during tectonic movements of natural or human origin [6,7]. Currently, we are facing one more aspect, which is ecology and sustainable construction. The sustainable industry is a series of activities aimed at reducing the negative impact of buildings on the environment throughout their life cycle, starting from the preparation of the design through the construction process to operation and demolition, concerning social, ecological, and economic aspects [1–8]. In 2011, “Roadmap to a Resource Efficient Europe” was published by the European Commission’s Communication. On the one hand, a high consumption/extraction of natural resources has been identified in the construction sector, and on the other, there is a large potential for prospective savings. A sustainability assessment carried out in accordance with these new standards quantifies the environmental, socioeconomic impacts and aspects of buildings as well as building elements using quantitative and qualitative indicators. In the field of construction products, the importance of this problem increases with the inclusion of the seventh essential requirement in the CPR (Regulation (EU) No 305/2011 of the European Parliament and of the Council—CPR), which assumes the gradual creation of EPDs = environmental product declarations, where the basic tool is also LCA [9–12].

Green sustainable construction is an essential tool in the fight against the climate crisis. The construction industry and buildings are responsible for 20–50% of natural resource use and nearly 40% of urban emissions [13]. The current concentration of carbon dioxide ( $\text{CO}_2$ ) in the Earth’s atmosphere is far too high and has reached the limit of 412 parts per million (ppm). This represents a 47% increase since the beginning of the Industrial Age, when the concentration was near 280 ppm, and an 11% increase since 2000, when it was near 370 ppm. Scientists know the increases in carbon dioxide are caused primarily by humans [14], and also humans should be able to stop the destructive impact of industrial activities on the environment. A beneficial aspect of demolition as part of sustainable development would be the recycling of materials, e.g., in the form of aggregate from used bricks. In connection with the above, sustainable development goals are based on decades of work by countries and the United Nations, including just stopping the destructive changes flowing on the part of the construction industry, despite the fact that it promotes improving the comfort of life, stopping climate change (gardening heat loss in buildings, modernization of combustion methods, or processing of building components in metallurgical furnaces). The UN Department of Economic and Social Affairs states that it is necessary to end poverty and other deprivations, improve health and education, reduce inequality, and spur economic growth—all while tackling climate change. The 2030 Agenda for Sustainable Development was adopted by all member states of the United Nations in 2015 and provides a common plan for peace and prosperity for people and the planet, now and in the future. One of the main aspects of the principles of sustainable development and construction is the reduction in overproduction and excessive exploitation of natural resources—including quartz sand [15]. Currently, environmentally friendly solutions are being introduced to the market that can relieve natural deposits of mineral resources. The materials from which the structural walls are made should also meet the standards of WT 2021 (Technical Conditions 2021). In accordance with the sustainable construction policy, the basic thermal criterion must be met:  $U_c \leq U_{c(\max)} = 0.20 \text{ W}/(\text{m}^2 \text{ K})$ , due to the fact that the external wall is an artificial partition between the external environment (variable temperature and humidity) and the interior (at a certain temperature and humidity) [16] and constitutes a material conducive to the accumulation of heat in rooms [17], which in turn is associated with the porosity of materials and microstructural changes that may occur in a naturally exploited

material. However, in the case of construction materials, the insufficient value of the heat transfer coefficient can be composed of a thermal insulation material.

Quartz sand ( $\text{SiO}_2$ ) is a material with a crystalline structure and is not very reactive, unlike components with an amorphous structure. Sand ( $\text{SiO}_2$ ), which is the most common form of silicon dioxide, is composed largely of minute quartz crystals and has a tetrahedral crystalline structure [18]. Sand extraction strongly interferes with the environment [19,20], because when it is extracted from rivers, lakes, or oceans, the coastline recedes. Since 2008, up to 90% of the world's beaches have shrunk by 40 m on average. According to estimates, 24 Indonesian islands disappeared under water between 2005 and 2014, and 80 others are at risk of being flooded. Analysis conducted for several years suggests that in the world, the excessive use of sand is starting to be felt. Sand is also imported by the desert countries of the Middle East, mainly due to the fact that not every type of sand is suitable for construction, and  $\text{SiO}_2$  [21] is the main element of building materials (concrete and bricks). Therefore, sand is the world's second most consumed natural resource [1,22]. Currently, it is consumed more than oil [23]. Zhong X. [24] from Leiden University, Netherlands, calculated that global demand for building sand will increase from 3.2 billion tons per year in 2020 to 4.6 billion tons in 2060, with Africa and Asia [25]. However, there are ways to reduce the extraction of sand from bodies of water by crushing rocks, recycling concrete or bricks at the end of their service lives and crushing glass bottles [23]. An important feature of the economy and sustainable construction is the interpenetration of various fields and sciences, including social and natural ones, in order to shape a suitable future for the next generations and to care for natural resources. For this reason, one of the solutions favoring this trend is the use of glass in the form of sand (from crushed bottles glass). This type of research has been conducted for at least a decade [26–34]. The purpose of this article is to analyze the possibility of using glass sand as a substitute for quartz sand in the production of materials resulting from hydrothermal treatment (so-called silicate bricks), because glass is another form of  $\text{SiO}_2$ , but its atomic structure is amorphous or irregular rather than crystalline [18]. Waste glass in concrete and other building materials has advantages and disadvantages. According to a U.S. Environmental Protection Agency report, the total amount of waste material has increased from 88 million tons in 1960 to 262 million tons in 2015. Glass is a material that can be recycled, but only colorless glass can be reused, for example, in the production of bottles. Colored glass, due to the content of impurities and derivatives, remains an unused material. It follows that only 34% of glass waste was recycled. In addition, it can be said that the recycled glass component can actually be used only twice—once for the production of bottles, and again as waste for disposal, e.g., in bricks, concrete, or other building materials [35].

The article is a review of the research conducted since 2016 on laboratory tests on the modification of silicate mass by glass sand (GS) from recycled bottle glass, the properties of the mass modified in this way (hydration temperature, consistency, and humidity of the mixture), physical and mechanical properties, structural, and potential durability, which are related to, e.g., the direction and degree of crystallization of the amorphous C-S-H phase [2,36–40]. The essence of the research is also the application of the geochemical modeling code in the process of analyzing the modification of silicate mass with glass sand. The basis for the appropriate functional properties of building materials is their internal structure, which changes as a result of weather conditions and an often aggressive environment. Based on the XRF analysis, the GEMS-PSI program (Gibbs energy minimization software for geochemical modeling) allows you to determine the potential process of crystallization and changes occurring in the material during operation [37]. Thanks to this proposition, it is possible to reduce ineffective modifications, and thus save time, money, and energy. Glass is one of the most complex materials ever observed on Earth.

The development of materials engineering research and advances in materials science have further increased the interest in glass and glass components.

Quartz sand is defined as a granular substance resulting from the erosion of siliceous rocks—which are mineral formations made up mainly of  $\text{SiO}_2$  (silicon dioxide, quartz, or

granite) and does not have a strict chemical composition due to the deposits from which they are mined. In its solid state,  $\text{SiO}_2$  silica dioxide exists as a large molecular structure with strong chemical bonds binding it together, known as a covalent lattice. The melting point of sand is an order of magnitude approximately 1700 °C. When it is brought to a sufficiently high temperature, the structure of the sand breaks down to such an extent that it can become a completely different material—glass. Compared to the crystal structure of silica in sand, the elements in glass are more randomly arranged and more prone to breakage. Glass belongs to a subcategory of solids known as amorphous solids, which also includes plastics, rubber, and asphalt [41]. Accordingly, fused silica is  $\text{SiO}_2$ , which is amorphous  $\text{SiO}_2$  with no impurities [42,43]. Tests described the beneficial aspects of using recycled waste glass as a partial replacement for sand in concrete [35,44–47]. A series of tests were carried out to determine the properties of the ingredients, fresh concrete and hardened concrete, including durability characteristics, in order to investigate the suitability of using recycled glass sand in concrete. It was proved that concrete, which was produced by replacing natural river sand with recycling in the amounts of 20%, 40%, and 60%, respectively. The study used multi-colored soda-lime glass collected by the Cairns Regional Council in Australia. The test results showed an improvement in concrete strength. Concrete with glass sand also showed better resistance to chloride ion penetration and reduced expansion caused by the alkali-silica reaction [44]. Another study investigated the potential use of waste recycled glass and pozzolanic glass powder [30,45], where no major differences in the compressive strength of concrete were found in the presence of glass sand as a substitute for quartz sand. It was described that the use of glass sand as a substitute for quartz sand in concrete carries a risk of expansion, as evidenced by cracks in the modified concrete. In order to minimize the phenomenon of ASR expansion (reaction of alkali with aggregates rich in reactive silica [46] in concrete modified with glass cullet, as the so-called ASR silencers, materials such as ground granulated blast furnace slag, metakaolin, and lithium nitrate ( $\text{LiNO}(3)$ ) were used [30,45–47]. As it has been proven, the color of the glass is also important when modifying building materials with waste glass. Mixed-color recycled glass waste is a material that cannot be reused in the glass industry. Concrete can be considered the starting point for surplus glass recycled from mixed-colored waste. Strong segregation was observed during the modification of recycled glass sand concrete, and the plastic properties of the concrete changed significantly [45]. Tagnit-Haomu [48], as one of the pioneers, used powdered colored glass bottles (considered as waste) in the modification of concrete. After processing, he used bottles in the form of glass powder, because the dust produced by grinding bottles is a pozzolanic material. The field trials summarized in this article confirm that concrete mixes produced with GP (glass powder) as a 10–30% replacement for Portland cement have good mechanical properties and high durability. This type of research was carried out on slabs of concrete inside buildings and on external slabs (pavements) subjected to an aggressive environment and cycles of freezing and thawing [47,48]. The use of waste glass powder (GP) in sustainable cement and concrete is justified as GP is rich in amorphous silica (~70%). In addition, the addition of GP affects the porous structure of the material, which plays a key role in the mechanical and durability properties of cement and other building materials. According to the analyses, the use of 30% GP in the raw material mass increased the total porosity of the mortar, which could also be influenced by the irregular shape of the pores and the fragmentation of the pore structure [49]. Other studies show that the addition of glass powder (WGP) contributed to the workability but led to an increase in the setting time of the resulting mass (OPC paste) [50]. It seems important to test the ECO-cement, where it was proved that large amounts (up to 70%) of Portland cement clinker in ECO-cement can be replaced with waste glass. According to the research results, the developed ECO-cement with 50% of waste glass possessed compressive properties at a level similar to normal portland cement [51].

An important aspect of using glass sand is also the structure of the glass itself. Glass sand has an amorphous, unstable (chaotic) structure and is a metastable material, so it

can crystallize. On the other hand, quartz sand used in silicate materials has a crystalline structure, so it is less reactive and resistant to temperature [37,52]. Due to the content of sodium oxide and the influence of hydrothermal conditions, the crystallization of the C-S-H phase takes place in the direction of the tobermorite [53] or gyrolite and natrolite phases [36,52–55].

In the construction industry, other modifications are also currently used that are based on the recycling of rubber mats or used tires. One research approach is the possibility of replacing standard construction materials with alternative, waste materials, such as waste rubber, and another research approach assumes extending the life of the pavement (disposal of waste rubber in a cement-stabilized subbase) [56]. Nonbiodegradable waste tires release toxic chemicals into the surrounding environment in landfills and landfills, with approximately 1.5 billion of them being produced annually worldwide. Used as a sand substitute in liquid concrete fill, rubber crumb improves ductility and strength-to-weight ratio. The tests showed that the concrete mix weighing 40 MPa with 0.6% rubber crumb content was characterized by optimal strength and aeration capacity, showing minimal damage after 56 freeze/thaw cycles. Rubber, as a partial substitute for aggregate in subbase and road subgrade layers, however, has a negative impact on the California load factor of the graded aggregate base course. In turn, mixtures of rubber and soil as a contact point between the foundation and the structure gave a 60–70% reduction in the vertical and horizontal accelerations of the ground after subjecting it to earthquake simulation modeling [57]. Another study was an experiment on uniaxial compression, uniaxial splitting, pure shear, and compression size effect of rubber concrete with five different substitution rates by applying hydraulic servo and direct shear apparatus. Their research showed that as the sample size increases, the integrity of the rubber concrete after damage gradually improved. Under the influence of the increased rate of rubber replacement, the strength of concrete to uniaxial compression, splitting tensile strength and shearing gradually decreased, and the plastic deformation capacity increased. As a result of the experiments, it was also found that the compressive strength was reduced by 60.67%, the shear strength by 49.85%; and uniaxial splitting strength by 58.38% [58]. Zheng W. and all investigated the possibility of using mat rubbers as stabilizing underlays for the tracks. Tests have shown that for a ballast-free track with an insulating layer made of a rubber mat, the maximum tensile deformation in the thickness direction does not exceed the initial compression of the rubber mat under the self-weight of its structure. Gaps and voids between the layers can be eliminated by pre-pressing the rubber mat [59].

The above studies are significant for the construction industry, environmental development, and sustainable economy, but they do not include the crystallization process that occurs as a result of hydrothermal treatment in which sand-lime bricks are produced, therefore, the article focuses on recycled glass sand and its course crystallization in hydrothermal conditions.

## 2. Materials and Methods

Material composition solutions should take into account the properties of the silicate mass, its optimal composition (consulted and tested), final amount and method of the modifier dosed. The standards were used: CEN. PN-EN 772-1: 2011E, CEN. PN-EN 772-13, 2001, CEN. PN-EN 1996-2: 2010, CEN. PN-EN 771-2, PN-EN 1936: 2010, PN-EN 993-1: 2019-01 [60–65]. The research methods included chemical, structural and microstructural studies of silicate bricks, which are characterized by a low content of quicklime (7% by mass) and rich in silica up to 90% by mass, which were modified with broken amorphous glass in the form of sand (GS). Tests of the oxide composition showed an increased content of sodium compounds [60–64]. The scope of the work presented in this article included the preparation of traditional and sand-modified building materials along with the determination of their mechanical characteristics using Statistica 10.0 program [66–68]. The tests of the structure and microstructure of autoclaved products were based on the following tests:

- physical and mechanical properties (compressive strength, bulk density, water absorption, porosity);
- Micro-CT analysis;
- SEM analysis to visualize the microstructure of the modified material;
- XRD analysis (X ray diffraction analysis) to determine the phase composition of traditional and sand-modified material;
- XRF analysis to investigate the elemental composition of glass sand;
- Simulation of geochemical modeling and application of GEMS-PSI (Gibbs Energy Minimization Software for Geochemical Modeling) [69].

Micro CT analysis was performed on a Nikon XT H 225 ST CT scanner (day of production: November 2018, UK). The CT scan was conducted with a reflection lamp (reflection target). The maximum capacity of this lamp is 225 kV and 225 W. The scan was made without a filter at 180 kV and 139 uA current. The exposure time is 250 ms. 4476 projections were made and assembled into a 3D model. Each projection was generated with 4 frames per projection. The size of the voxel, i.e., the resolution, is 15  $\mu\text{m}$ . All parameters have been selected experimentally to ensure the best image quality. During the CT scan, the pores were determined using the porosity/inclusions analysis tool in VG Studio Max [16]. Porosity research were performed using a QUANTACHROME ULTRAPYC 1200e helium pycnometer (Micromeritics Instrument Corporation, Norcross, GA, USA) on irregularly shaped samples weighing approximately 10–25 g. The helium pycnometer used in this test is a fully automated piece of equipment [36].

The phase compositions and structure for both materials (with QS and GS) were examined employing the X-ray diffraction (XRD). The photos presented in the article were taken on three kind of Scanning Electron Microscope analyses (FEI Nova NanoSEM<sup>TM</sup> 230 microscope with field emission gun and variable pressure capabilities, IROL 5400 working with the EDS analyzer, equipped with a Thermo Scientific<sup>TM</sup> NORAN<sup>TM</sup> System 7 and QuantaFEG, FEI Company). XRD phase analysis was performed in the range of 5–70° 2θ. Qualitative identification of the phase composition of the samples was carried out on the basis of the ICDD PDF-2 database [36,38].

Mechanical and microstructural tests were conducted for samples after 36 months from the production time of bricks containing glass components in the range of 0–90 wt% glass sand (GS). For the microscopic examinations, samples with 0 wt% GS and 90 wt% GS were used. The microstructure using a scanning electron microscope was also examined after 6 years (in 2022) from the date of production of the material (in 2016).

## 2.1. Materials

In modern construction, glass is one of the basic materials willingly used by an architect, constructor or technologist. The launch of glass production in Italy in 1241 (in the first stage as the production of mirrors) contributed to the popularization of glass. In the 16th century, there were already 30 glassworks, and the industrial production of glass dates back to the end of the 19th century [70]. Glass (Figure 1), as a material, is a transparent, non-crystallized and inorganic substance that is formed as a result of melting glass raw materials at a temperature of 1300  $\div$  1500 °C, and the raw material used for its production is pure quartz sand. Pure silica, melting, creates pure glass with beneficial properties (including: high softening point, chemical resistance, high resistance to sudden temperature changes) [71]. Sands used for the production of glass must be of very high purity and grain size 0.1  $\div$  0.15 mm and are introduced in the amount of about 70–72%. To lower the melting point and viscosity of the mass, so-called fluxes, or carbonates ( $\text{Na}_2\text{CO}_3$ ,  $\text{K}_2\text{CO}_3$ ), are added. In order to change the properties of the glass, the main components of the glass are replaced with other oxides, thus obtaining different types of glass [70]. Under the scanning electron microscope (SEM), glass is characterized by a uniform, compact structure (Figure 1).

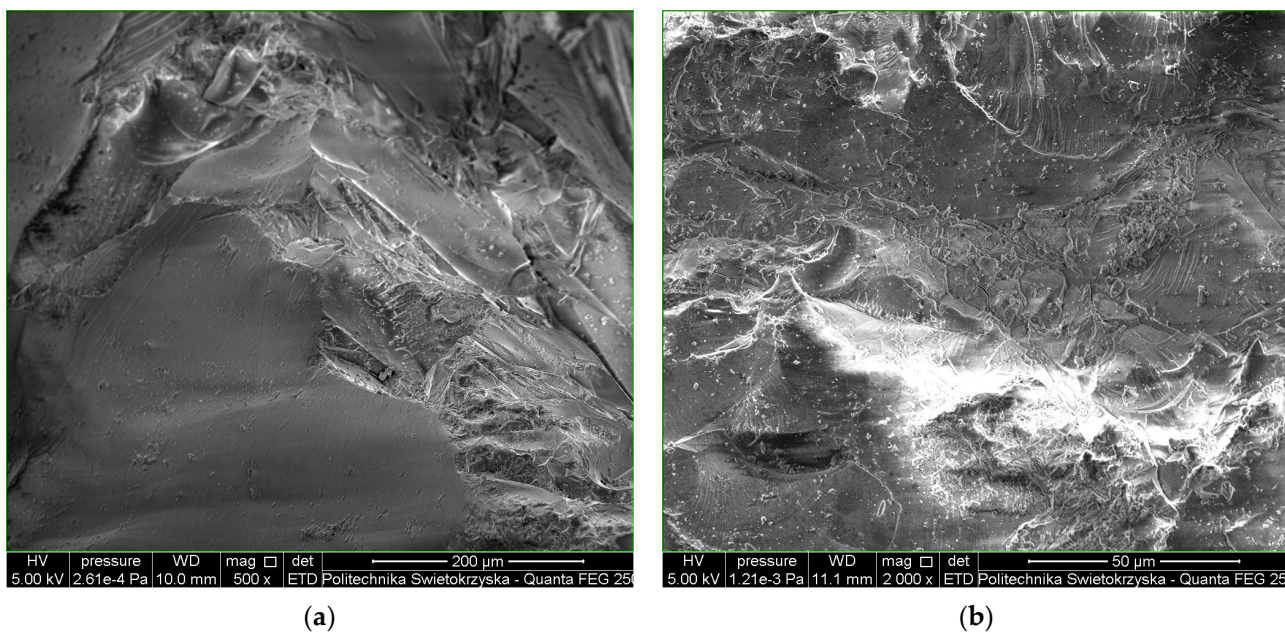


**Figure 1.** Examples of glass microstructure from recycled bottles observed under a scanning electron microscope (SEM); (a) colorless bottle glass, 200  $\mu\text{m}$  magnification; (b) white bottle glass, 50  $\mu\text{m}$  magnification.

Quartz sand has a crystalline structure, i.e., an ordered, smaller specific surface and is less reactive in relation to recycled glass sand, which is characterized by an amorphous structure (disordered, chaotic, an example is glass sand used in the tests presented in the article or fly ash generally used in the modification of concrete) and, such as amorphous phases (C-S-H), also has a larger specific surface.

Photo Figure 2 shows a brick made of quartz sand (QS). Figure 3 shows an image of the microstructure of the same brick.

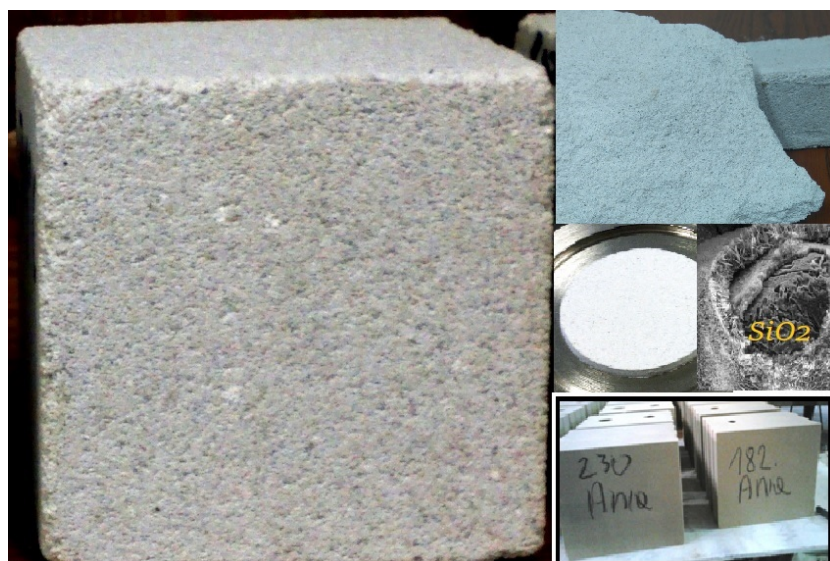


**Figure 2.** Traditional (reference) silicate brick: a brick with dimensions of 5  $\times$  5  $\times$  5 cm and a break through the structure of the brick.

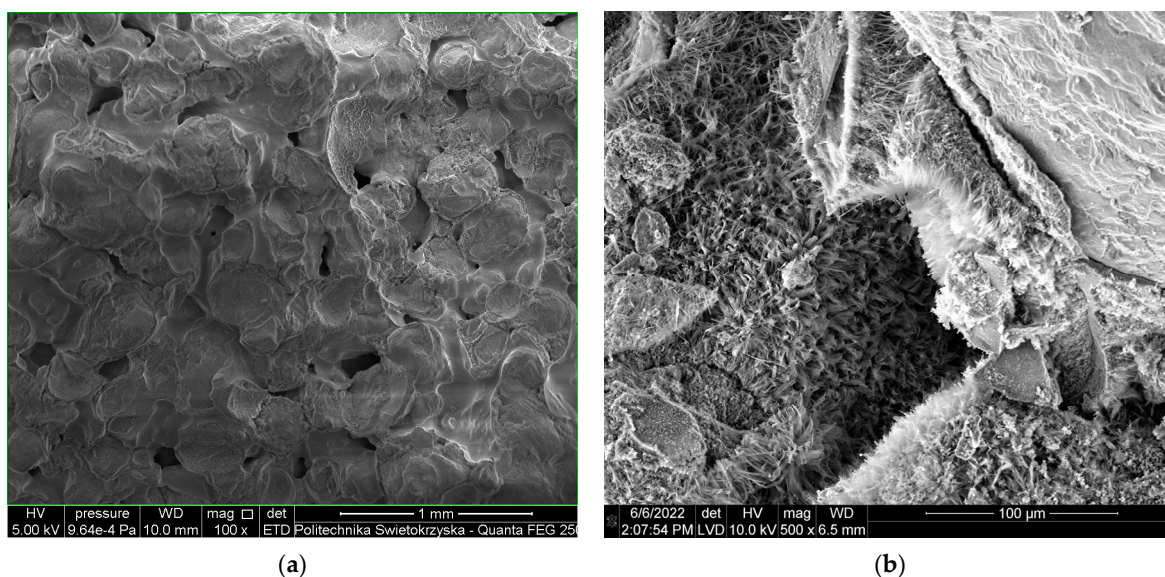


**Figure 3.** Traditional (reference) silicate brick observed under a scanning electron microscope (SEM); (a) microstructure of the material after 36 months from the production of traditional silicate bricks produced in industrial conditions, 1 mm magnification; (b) the microstructure of a reference brick produced in industrial conditions after 20 years from the date of production, 100  $\mu\text{m}$  magnification.

C-S-H is a phase which is responsible for the development of strength in concrete. It is an amorphous phase that crystallizes over the years [31–33]. At the moment of crystallization of the C-S-H phase, its specific surface changes (decreases) creating free spaces in the pores, which allow, for example, water to interfere with the concrete structure, which in turn leads to the destruction of the concrete structure (or other groups of building materials, such as autoclaved bricks). That is why it is so important to study the structure of amorphous sand and hence materials modified with amorphous glass components to determine their durability under environmental changes (temperature,  $\text{CO}_2$  concentration in the atmosphere) and to compare the microstructural features with the physical and mechanical features of the materials modified in this way [27,34–38].

The silicate mass for the production of laboratory bricks (Figures 2 and 4) was composed of: quartz sand ( $\text{SiO}_2$ ) or glass sand (GS) + binder/quicklime ( $\text{CaO}$ ) + water ( $\text{H}_2\text{O}$ ). The sand used in these type of modification had a grain size ranging 0–2 mm (90% relative to the weight of the product, wherein 50–60% of the 90% that sand with a grain size of 0–0.5 mm, and the remaining 30–40% of the 90% present in the sand mass was sand with a grain size 0.5–2 mm. Glass sand had a grain size between <80–160>  $\mu\text{m}$ .



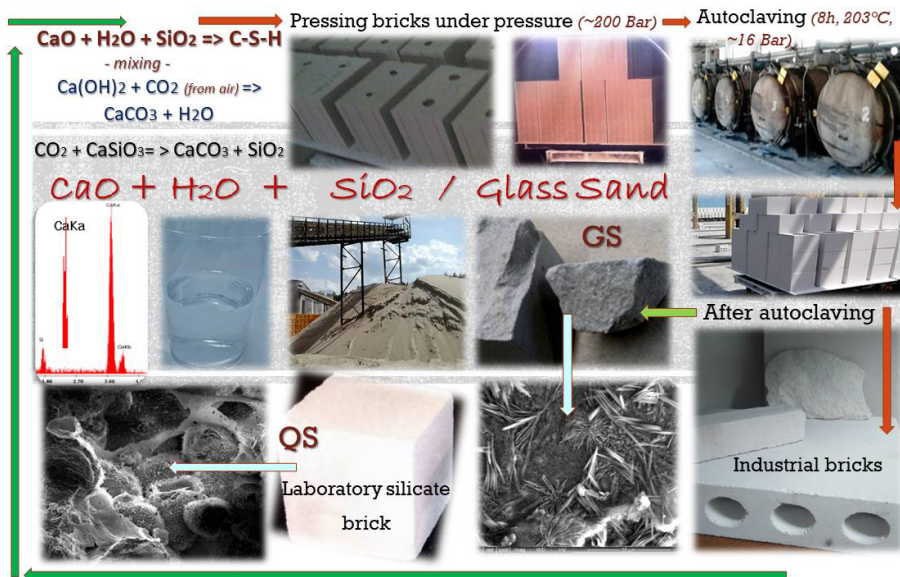
**Figure 4.** Silicate brick a brick with dimensions of  $5 \times 5 \times 5$  cm modified with recycled glass sand and a break through the structure of the brick modified by 90 wt% glass sand (GS).

The photos (Figure 3a,b) are a picture of a traditional material produced in industrial conditions and produced on the basis of quartz sand. The silicate material produced on the basis of  $\text{SiO}_2$  is resistant to weather conditions, as evidenced by the lack of changes in the microstructure of the material. This is due, among others, to the fact that this type of bricks is created under conditions of increased pressure and temperature. The fragment

to be examined under a scanning electron microscope comes from a building operated since 2003 in a temperate warm transitional climate [1]. Photo Figure 2 shows a traditional silicate brick made of quartz sand (QS), photo Figure 4 shows laboratory bricks made on the basis of glass sand (GS).

## 2.2. The Autoclaving Process and Characteristics of the Problem

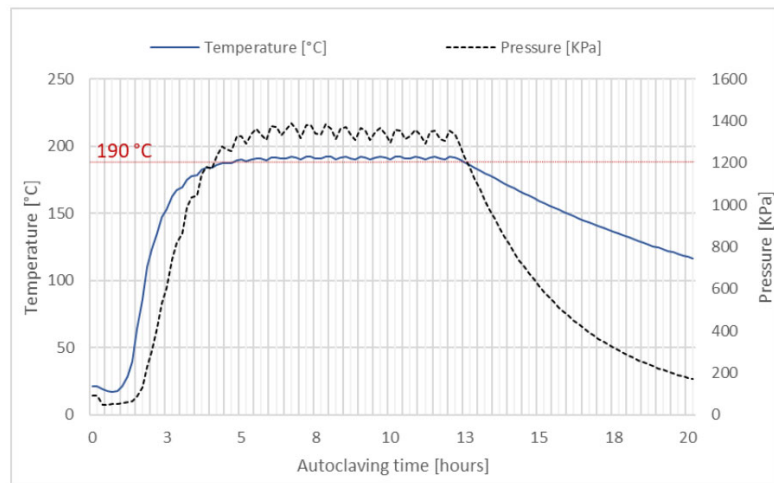
Traditional silicate bricks produced in industrial conditions (Figure 5) are structural building materials that are formed in hydrothermal conditions (at a temperature of about 200 °C under a pressure of 16 bar (1.6 MPa) Figure 6), and a visual diagram of their production is shown in Figure 5. The production of this type of bricks is mainly based on: sand ( $\text{SiO}_2$ : 87–90%), lime ( $\text{CaO}$ : 3–7%) and water ( $\text{H}_2\text{O}$ : 3–5%). There are also construction materials with increased acoustics, then they are modified with basalt aggregate [38,71–76]. The pre-prepared substrate mixture (sand, lime, water) is placed in steel reactors, where it remains for about 4 h. There, the lime slaking process takes place, accompanied by an increase in temperature to about 60–80 °C. The lime-sand mass is directed to the press, where it is compressed under a pressure of 15–20 MPa, and then formed under pressure into blocks of the appropriate size and shape. Hydraulic presses are used to produce these bricks. In the final phase, the pressed bricks are placed in devices called autoclaves and subjected to the hardening process. Within 6–12 h (average 8 h) of autoclaving,  $\text{CaO}$  enters into a chemical reaction with  $\text{SiO}_2$  and the mixture is recrystallized [37,38]. After the autoclaving process, the bricks are packed and stored on pallets.



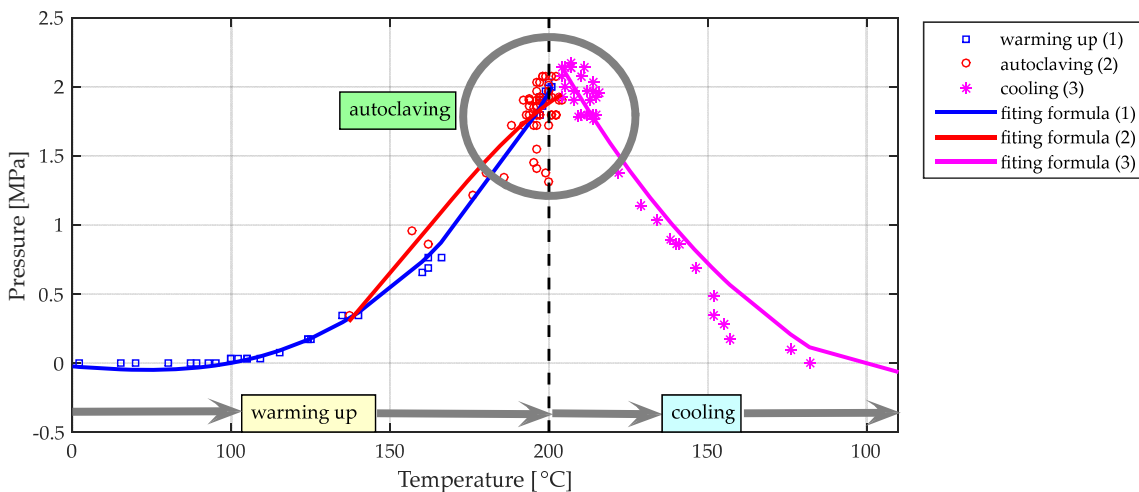
**Figure 5.** Production process of sand-lime brick in industrial conditions [16].

Figure 6 shows the autoclaving process in industrial conditions, while Figure 7 shows the autoclaving process in laboratory conditions (3 production trials). The autoclaving time was reduced up to 5 h (1 h heating and 5 h autoclaving and cooling (cooling down until the temperature drops to about 40–50 °C)) due to the limitation of the laboratory autoclave equipment. In laboratory conditions, in the autoclaving process, bricks with dimensions of 5 × 5 × 5 cm were manufactured. The autoclaving conditions shown in the chart were based on 3 independent tests during the production of silicate bricks in laboratory conditions. The Figure 7 shows the scheme of heating up the autoclave with the raw material (bricks) inside, then the autoclaving process (hydrothermal conditions: about 200 °C and pressure). After the proper autoclaving stage, the autoclave is cooled down in order to reduce the pressure and temperature (due to the danger associated with hot steam present in the autoclave, the device was left to cool down to a temperature of about 40 °C).

This process had a positive effect on the modified brick not exposing the material to rapid temperature changes).



**Figure 6.** Autoclaving process under industrial conditions [77].



**Figure 7.** Autoclaving conditions used in laboratory setting during the brick production (3 processes with 10 elements each).

### 3. Results

The tests and the presented tests were performed based on the CEN standards: PN-EN 772-13: 2001, CEN. PN-EN 1996-2, CEN. PN-EN 771-2. Basic examination methods included chemical and microstructural tests of the materials which contain low lime content 7% by mass and are abundant in silica up to 90% by mass and which were modified with broken amorphous glass (GS) containing higher levels of sodium compounds [60–65]. The raw material mix was prepared in two ways:

1. first, molds were made with the reference material (90%  $\text{SiO}_2$  + 7%  $\text{CaO}$  + 3%  $\text{H}_2\text{O}$ )
2. the subsequent molds contained the addition of glass sand (GS) until the quartz sand was completely eliminated (90% GS + 7%  $\text{CaO}$  + 3%  $\text{H}_2\text{O}$ ).

The tests of physical and mechanical properties are presented in steps of 10% of GS in the raw material mass. For the study of the microstructure of the materials, only a reference sample made on the basis of quartz sand only and a sample where the quartz sand was completely eliminated in favor of glass sand (90% GS) were selected.

The hydration temperature between the binder (lime) and water in the presence of quartz sand during the production of traditional brick is typically around 80–96 °C. How-

ever, the gradual elimination of quartz sand in favor of glass sand leads to a temperature reduction down to 39–42 °C with the use of 90% GS in the raw material mass.

### 3.1. Physical and Mechanical Properties and Usability of Modified Silicate Products

Based on the presented theoretical considerations and analyses based on laboratory observations, optimal solutions for the tested variants were determined due to the usefulness from the user's point of view. Desired ranges of the output size have been defined, i.e., compressive strength of silicate products modified by glass sand. For practical (engineering) reasons, the optimal value (Table 1) of compressive strength should be within the range of production construction bricks (15–20 MPa), and in the most favorable case, be higher than the value of traditional products (more than 20 MPa). The value of compressive strength is indicated to be greater than 15 MPa (Figure 8), which is the basic range for the production of autoclaved bricks and is a beneficial and useful value for the user (Figures 9 and 10). In addition, it is important because glass sand has different structural properties than quartz sand, and changes occur already at the stage of the hydration process (reduced hydration temperature to an average of about 40 °C in the case of replacing quartz sand (QS) with glass sand (GS)). However, the strength results are kept within the indicated optimal limits. In addition, the observation of laboratory bricks reveals a more compact, smooth and damage-resistant texture of bricks modified with glass sand and the crystallization of amorphous phases after 36 months from the production of bricks.

**Table 1.** Satisfactory size ranges for the criterion of optimizing the composition of silicate mass modified with glass sand (GS) as a substitute for QS quartz sand in the presence of water ( $H_2O$ ).

Criterion	Satisfactory Size Range		
	Short U = 0.00	Average U = 0.5	High U = 1.0
Compressive strength [MPa]	4.80	12.5	20.3

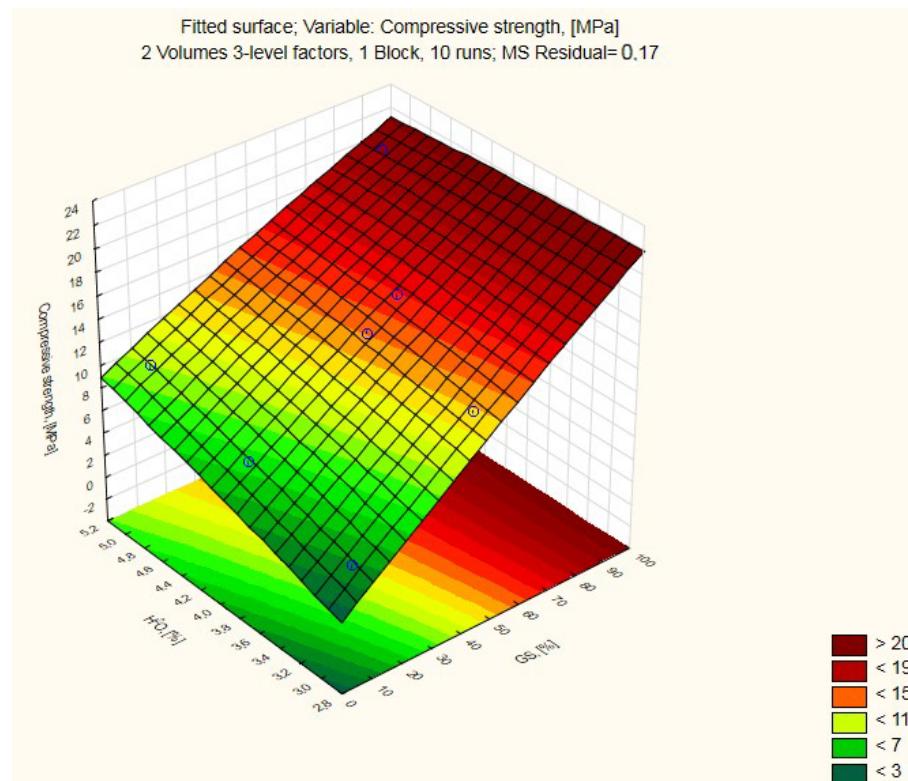


**Figure 8.** Compressive strength diagram for autoclaved brick modified with glass sand (GS) as a substitute for quartz sand (QS) in the presence of water ( $H_2O$ ).

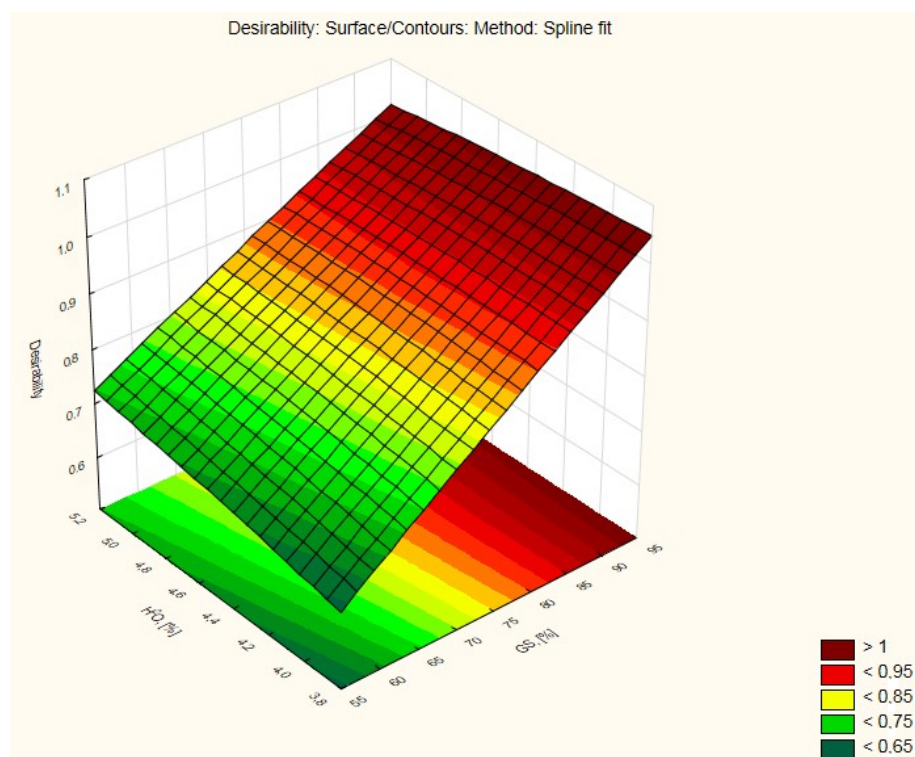


**Figure 9.** Graph of usability functions and their projection, with points of total usefulness (compressive strength) of silicate products modified by glass sand (GS).

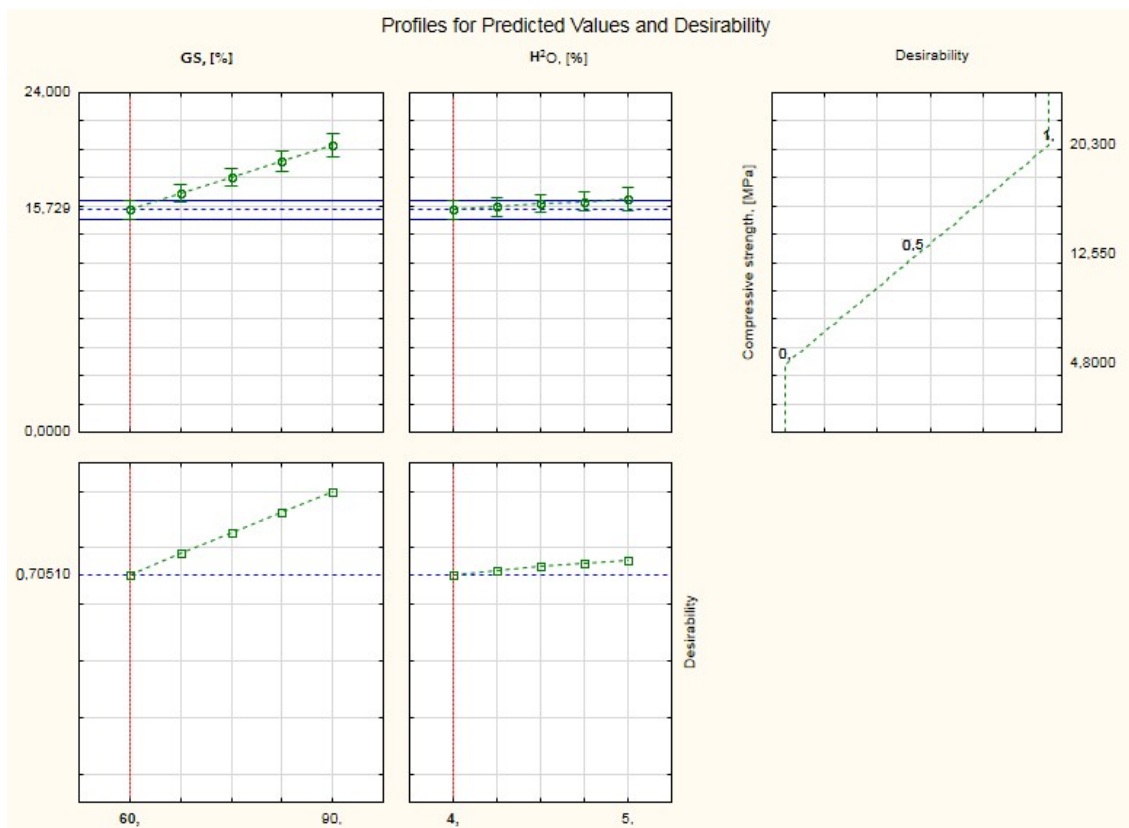


**Figure 10.** Total usability profile of silicate products modified with recycled glass sand (GS).

The user-relevant total utility graph (as the geometric mean of the partial utilities, Figure 10) confirms that the optimum glass sand content is 60% with 4% water, providing a compressive strength value of over 15 MPa (15.729 MPa) with a utility of approximately 0.71. The analysis confirms the expected effect of the modification. The remaining utility values for points on the grid corresponding to the input data are also shown.

Three types of samples were analyzed using a mercury porosimeter: AStTrad, i.e., a traditional (reference) brick bred in laboratory conditions, a silicate brick modified with 50% GS, and a silicate brick in which quartz sand was completely replaced with glass sand (ASt3L). The distributions of the Ast1 TRAD and Ast2 50% GS curves (Figure 11 [78]) are similar, which indicates that the uniform share of aggregate in the materials modified with glass sand shows properties similar to those of traditional silicate bricks. This is due to the optimal combination of quartz and glass sand. By increasing the amount of glass sand, the raw mass becomes plastic, and the mass itself acts, such as clay. The GS curve shows that pores with smaller diameters have a greater share in the material, and the share of pores with diameters above 1  $\mu\text{m}$  decreases. Mercury is forced to use a pressure of over 100 MPa with pores with a diameter of 0.01  $\mu\text{m}$  and smaller, which means that the sample of the tested material and the porous skeleton are unable to withstand such a load. As a result, some of the pores are destroyed under the influence of the forces (pressure) [78]. Figure 12 presents the dependence between compressive strength, bulk density, water absorption, and humidity of silicate autoclaved materials modified by glass sand in the amount of 0–90% of the total weight of the product. The maximum amount of sand in the mass is 90%. During mixing and mass preparation of silicate mass modified by glass sand, it was noticeable that the more water or the higher the humidity of the glass sand, the more the mass took the form of clay, and the water absorption of the material with glass sand depended on the amount of glass component and the amount of added water (limited to the amount of 3–5% water, as in the case of standard brick production).

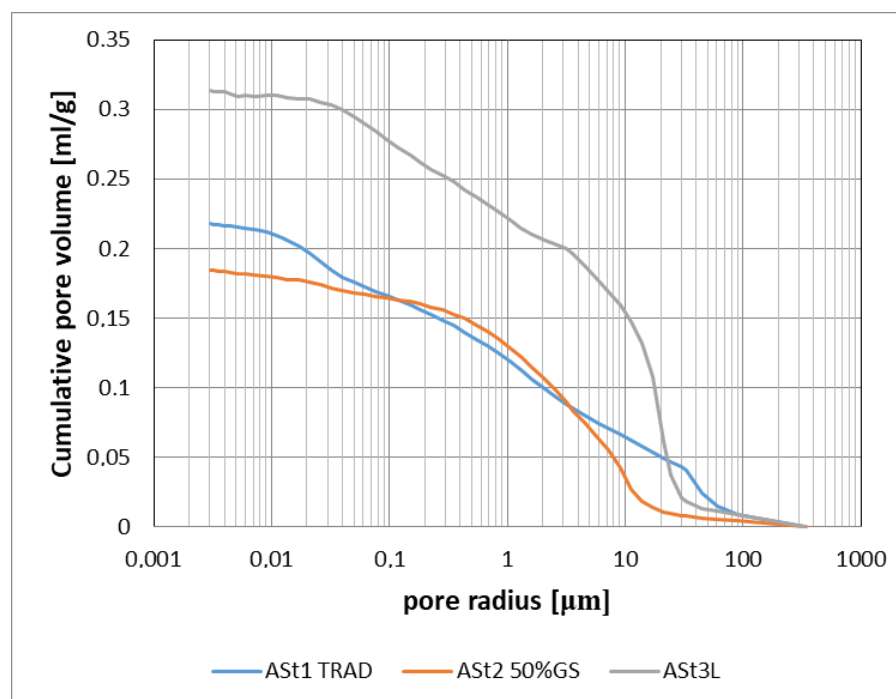


**Figure 11.** The cumulative volume of pores in the samples of silicate material: traditional (blue color), modified with 50% glass sand and 50% quartz sand (red color), and the material fully modified (90%) with glass sand (gray color) [78].

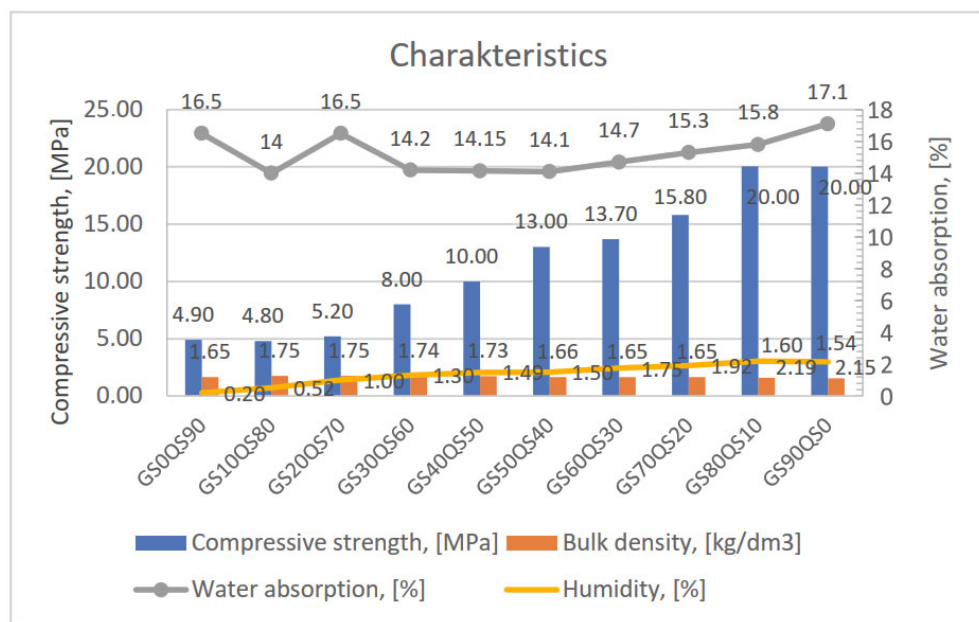


**Figure 12.** Dependence of compressive strength (blue color), bulk density (orange color), water absorption (grey line), and humidity (yellow line) of silicate autoclaved materials modified by glass sand (0–90% GS).

As the analysis showed, changes occur in the compressive strength, while the bulk density decreases with the increase in the share of glass sand, and the water absorption ranges from 14 to 17% but is maintained in the range of maximum water absorption for traditional silicate bricks (18%).

### 3.2. Internal Structure Analysis—Computed Tomography Method, Microstructure, Durability, and Geochemical Simulation

In order to visualize the arrangement of pores in the studied materials, the following analyses were performed: micro-CT analysis (Figures 13–15 for the reference brick together with Figure 16—photo of the microstructure of traditional brick and photos Figures 17–20—bricks modified by glass sand (GS)).

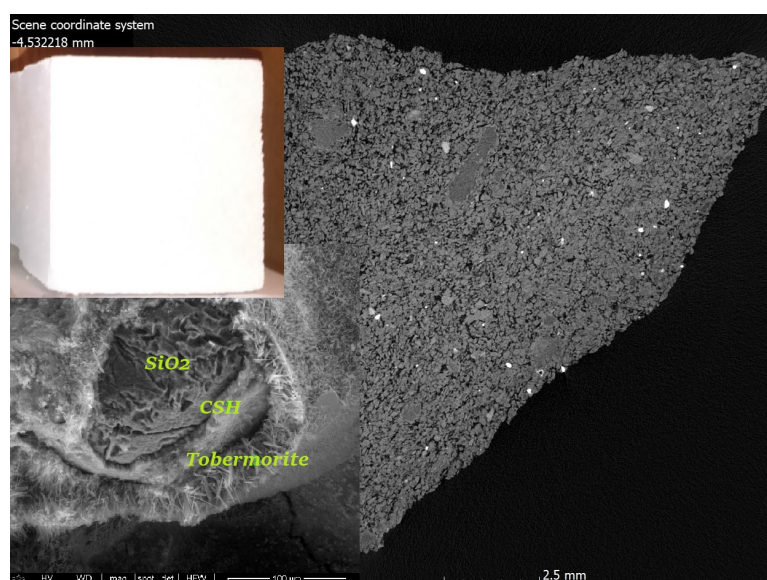


**Figure 13.** Computer tomography together with a photograph of the analyzed laboratory brick and an area of microstructure where a grain of quartz sand is visible.

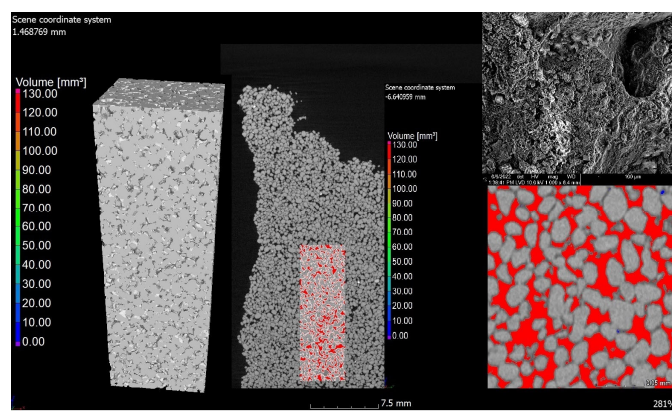


**Figure 14.** Computer tomography—an image and a three-dimensional cross-section through a sample of a traditional sand-lime brick with quartz sand (laboratory production).

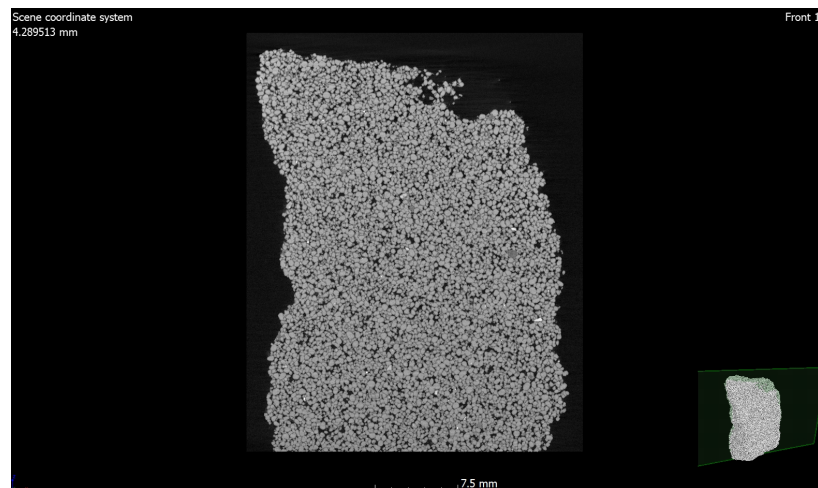


**Figure 15.** Image of the porous structure of traditional (reference) silicate brick with 90% QS.

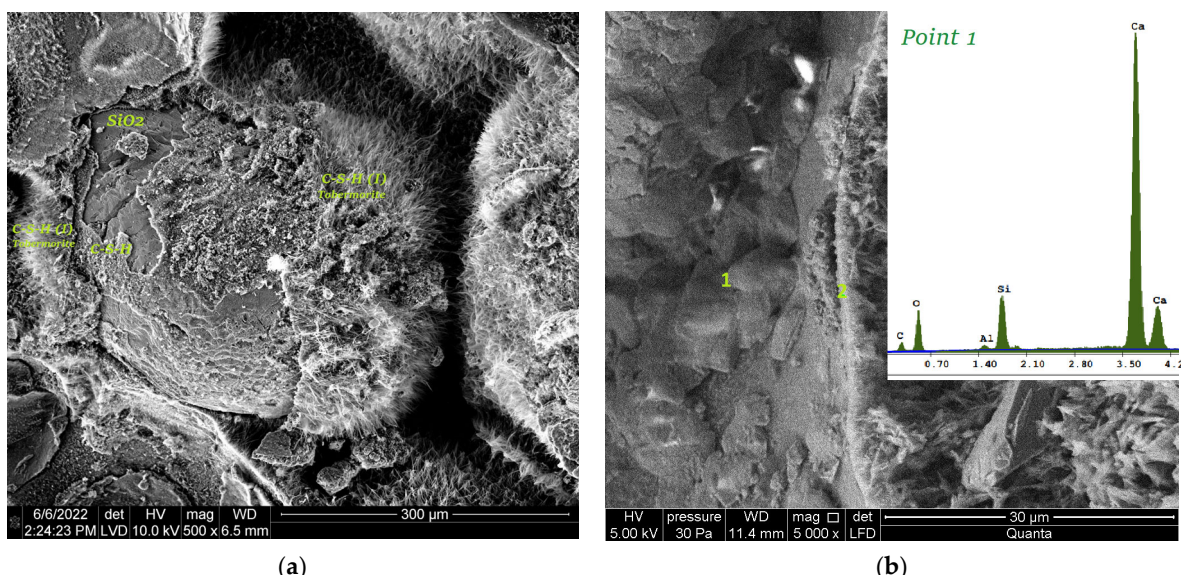


**Figure 16.** Microstructure of traditional (reference) silicate brick observed under a scanning electron microscope (SEM); (a) microstructure of the material 36 months after the laboratory production of traditional silicate bricks with quartz sand, 300  $\mu\text{m}$  magnification; (b) the microstructure of a reference brick with EDS spectrum, 30  $\mu\text{m}$  magnification.

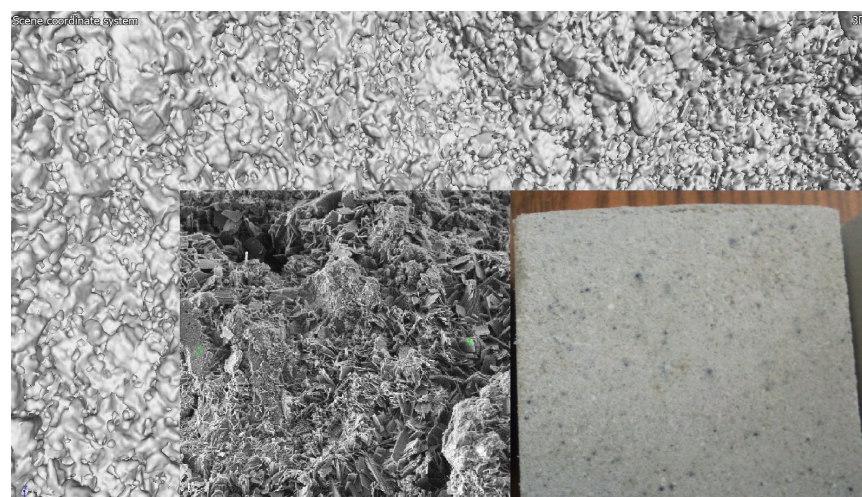


**Figure 17.** Computer tomography with a photograph of the analyzed laboratory brick and an area of microstructure (SEM, 50  $\mu\text{m}$ , brick  $5 \times 5 \times 5$  cm) of brick modified by glass sand.

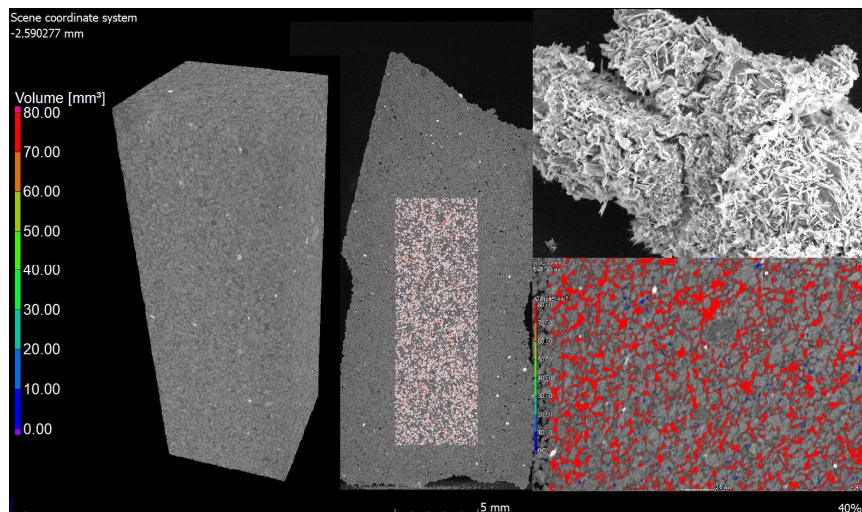


**Figure 18.** Computer tomography—an image and a three-dimensional cross-section through a sample of silicate brick modified by glass sand (90% GS, laboratory production).

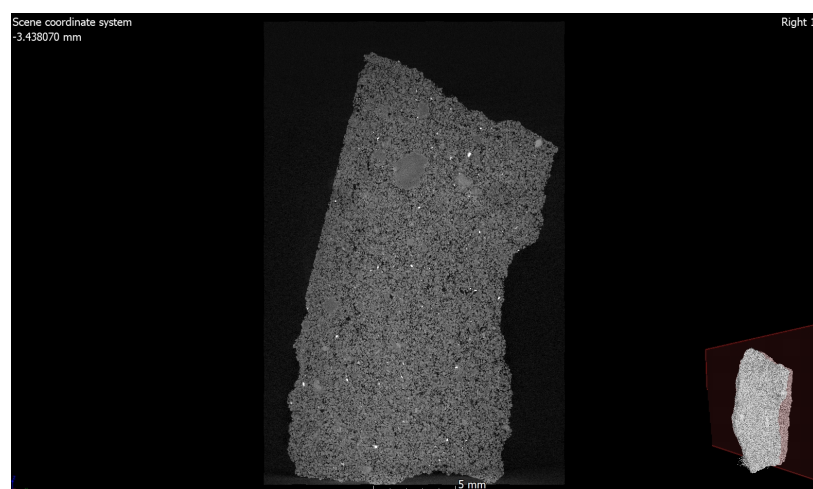


**Figure 19.** Image of the porous structure of silicate brick with 90% GS.

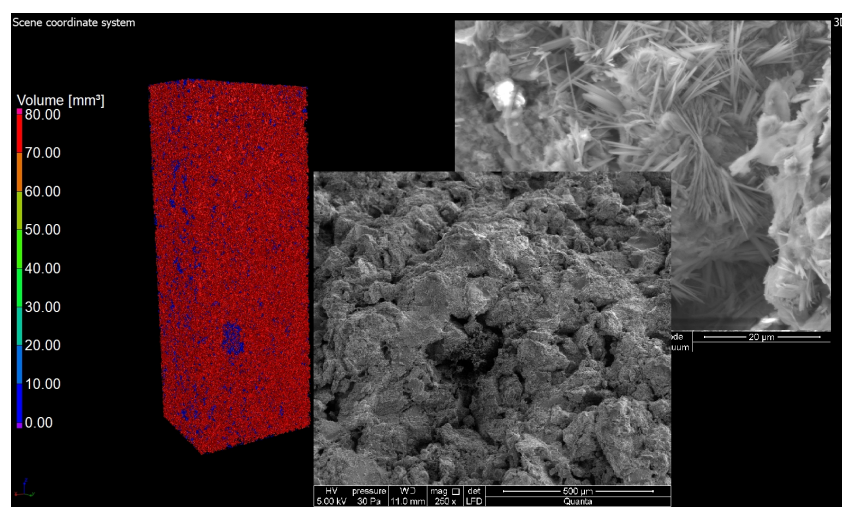


**Figure 20.** Cross-section through a sample of a brick modified by glass sand and a three-dimensional image of the porous structure of the material with the SEM images.

In order to separate the material from the voids, the value of the so-called voxel gray threshold was defined (the voids corresponded to the shades of black and very dark gray, and the remaining areas were material). All voxels corresponding to the darker areas were identified and counted, thus obtaining the percentage and volume of pore content of the entire sample volume as well as the volume of each individual pore (Figure 14). A computer tomographic study showed the volume of pores in a sample of a sample modified with glass sand within the limit of 23–30% of the analyzed area. This difference is due to the use of the boundary of the pores. Some pores have poor and vague boundaries within which they run (a very light shade of gray in the drawing), which is easy to overlook. These pores are damaged in the case of testing, with mercury thinning as a result of rapid injection into high-pressure porous mercury material [36].

Pores with diameters smaller than the obtained resolution cannot be detected. The research was supplemented by an analysis using a scanning electron microscope, which showed the size, method, and direction of crystallization and the form of phase structures occurring in autoclaved materials. Silicate bricks differ from concrete in that the structure of concrete consists of more than 60% of the volume of the solid formed from the calcium silicate hydrated phases, abbreviated as C-S-H (dominant phase, C-S-H phase is the main contributor responsible for the development of strength in hydrating cements). Amorphous calcium silicate hydrate ( $\text{xCaO} \cdot \text{SiO}_2 \cdot \text{yH}_2\text{O}$ ) is a poorly crystalline thermodynamically metastable product of variable composition in terms of its  $\text{H}_2\text{O}/\text{SiO}_2$  ratio and Ca/Si molar ratio [27,32,37,40], while autoclaved bricks consist mainly of the tobermorite phase or other crystalline phases (depending on the modification method and the modifier itself, Figure 16). In the case of glass sand, the direction of crystallization is towards gyrolite or natrolite. Due to the presence of magnesium oxide and depending on the temperature and operating conditions, it is also possible to form the M-S-H phase instead of the C-S-H phase [69,79].

The photos (Figures 17–23) show the internal structure (arrangement and porous material characteristics and microstructure) of a silicate brick modified with glass sand and produced in laboratory conditions (autoclaving time: 5 h, temperature: approximately 200 °C).

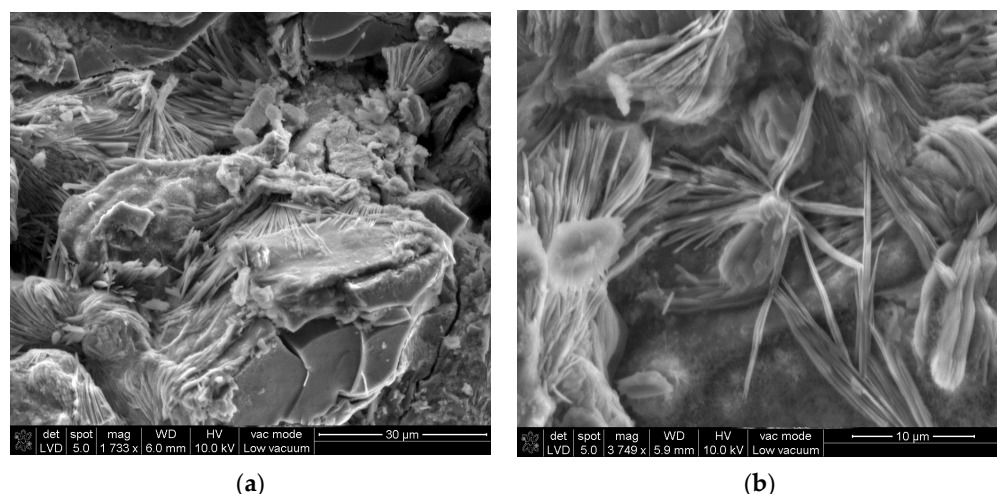


**Figure 21.** Microstructure of silicate brick modified by glass sand (50%) and quartz sand (50%) observed under a scanning electron microscope (SEM); (a) microstructure of the material after 36 months from the laboratory production, 30 µm magnification; (b) microstructure of the material after 36 months from the laboratory production, 10 µm magnification.

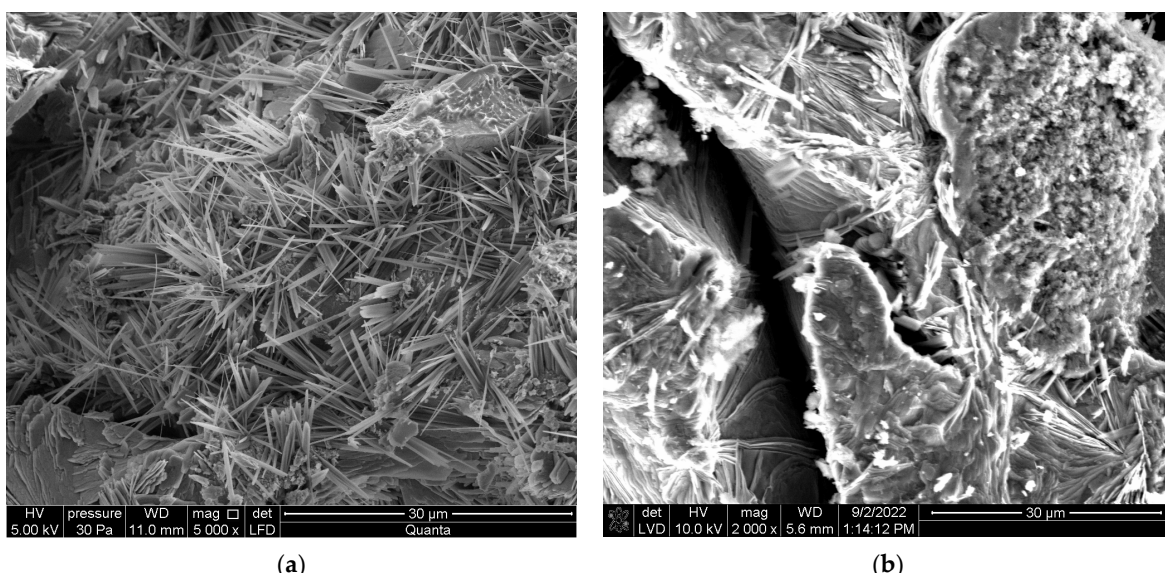


**Figure 22.** Microstructure of brick modified by GS (50%) and QS (50%); (a) microstructure of the material after 6 years (in 2022) from the laboratory production (in 2016), 30 µm magnification; (b) microstructure of the material after 6 years from the production, 30 µm magnification.

The photos (Figures 16 and 21–24) were created using a microscope SEM–FEI Nova NanoSEM, high vacuum. Due to the low binder (lime) content (3–7%) in the bricks and the above-mentioned hydrothermal conditions, the formation of C-S-H in sand-lime bricks is limited, and a crystalline low-calcium analog of C-S-H, called tobermorite is formed. Due to the relatively low calcium content in brick materials and the hydrothermal conditions, C-S-H formation in sand-lime bricks is minimal, and the C-S-H phase transforms into an analog of low calcium phases such as tobermorite (or otherwise known as C-S-H (I)). Recycled glass sand contains large amounts of sodium ( $\text{Na}_2\text{O}$ ) compounds that guide the crystallization process towards gyrolite [35,75]. Table 2 shows the EDS spectrum (analysis) at selected points for a brick based on glass sand (this supplement to Figure 23).

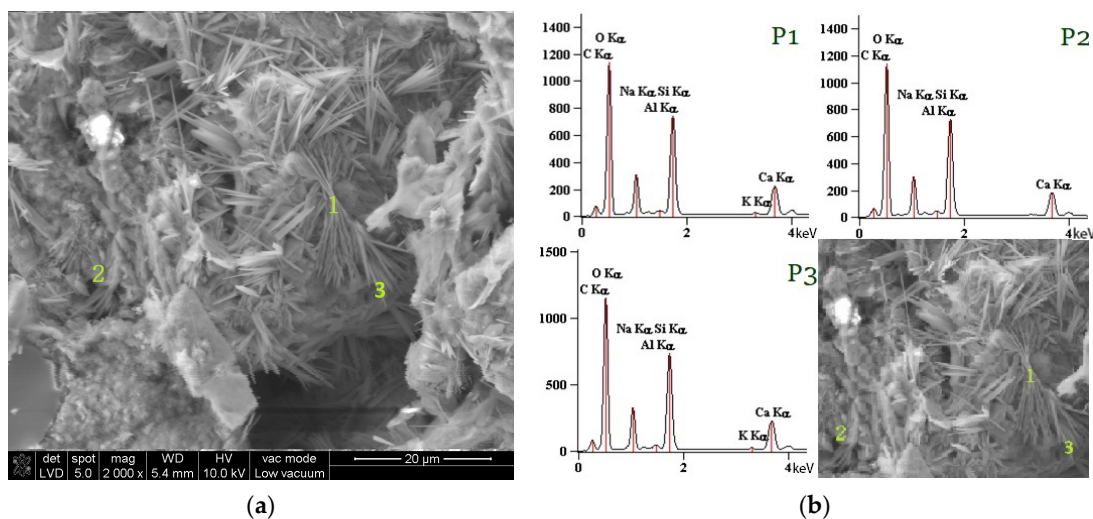


**Figure 23.** Microstructure of silicate brick modified by 90% glass sand 36 months after the laboratory production; (a) SEM image of brick modified by 90% GS, 20  $\mu\text{m}$  magnification; (b) EDS spectrum of brick modified by 90% GS at points 1, 2, and 3.

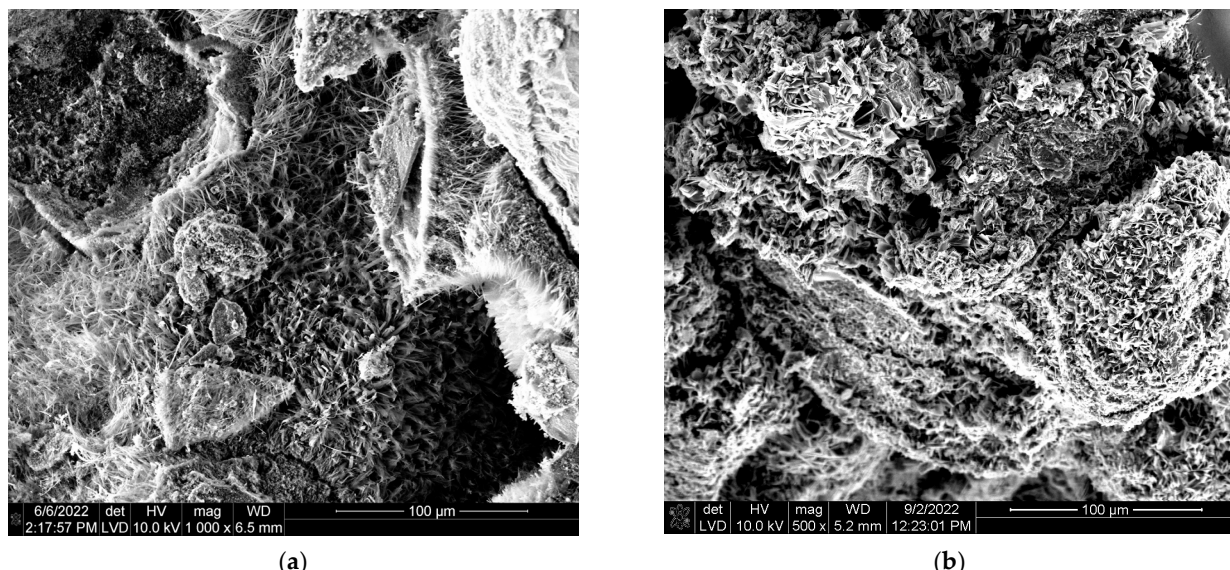


**Figure 24.** Microstructure of silicate bricks after 6 years (in 2022) from the laboratory production (in 2016); (a) microstructure of the laboratory bricks with 90% QS, 100  $\mu\text{m}$  magnification; (b) microstructure of the laboratory bricks with 90% GS, 100  $\mu\text{m}$  magnification.

**Table 2.** EDS analysis results for a brick modified by 90% GS (after 36 months).

	C-K	O-K	Na-K	Mg-K	Al-K	Si-K	K-K	Ca-K
90GS(6)_pt1	458	8300	2290	-	234	7014	114	2834
90GS(6)_pt2	478	8455	2267	-	259	6872	-	2246
90GS(6)_pt3	566	8668	2476	-	248	6959	173	2682
90GS(6)_pt1	$\pm 35$	$\pm 96$	$\pm 67$	-	$\pm 31$	$\pm 100$	$\pm 28$	$\pm 59$
90GS(6)_pt2	$\pm 23$	$\pm 92$	$\pm 65$	-	$\pm 32$	$\pm 100$	-	$\pm 53$
90GS(6)_pt3	$\pm 25$	$\pm 93$	$\pm 66$	-	$\pm 32$	$\pm 101$	$\pm 28$	$\pm 100$

XRD tests were performed on samples made 30 days after the date of production of the materials. The research was carried out for the traditional (reference) sample containing quartz sand (Figure 25a) and next for the sample modified by glass sand (Figure 25b). The area of each sample was swept by an electron probe at a voltage of 5–50 keV. On the basis of

the images obtained, the analysis of the microstructure and the determination of the phase composition was possible. Industrial quartz (QS) and glass sand (GS) were used to modify the bricks. The XRD phase analysis of the traditional brick and brick modified by GS samples was performed in the 5–70° 2θ range. The qualitative identification of the phase composition of the samples was performed with reference to the ICDD PDF-2 database [38].

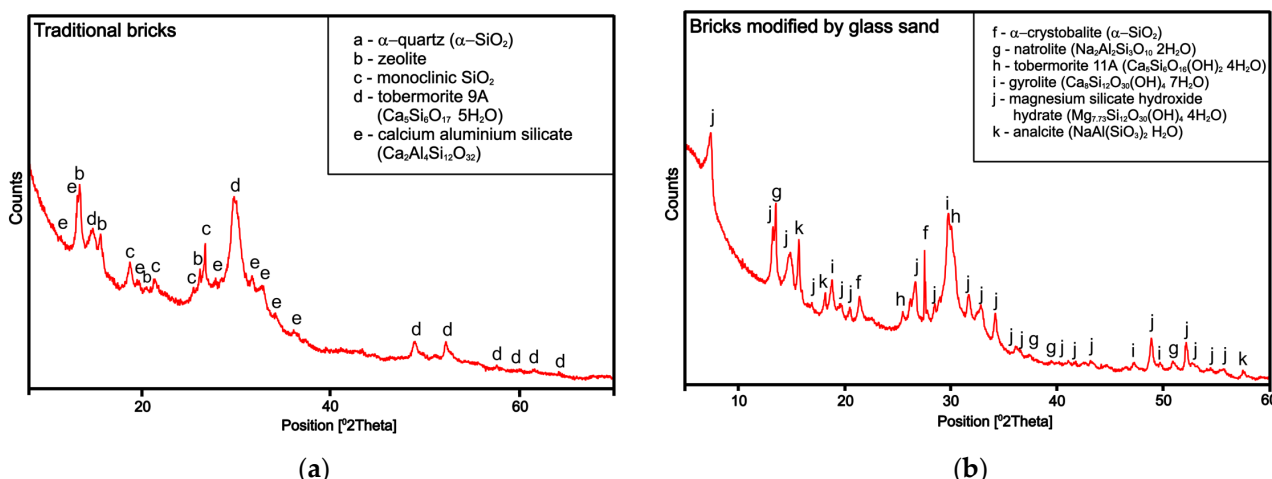


**Figure 25.** (a) XRD of reference sand-lime sample containing quartz sand (QS); (b) XRD analysis of the bricks modified by 90% GS after 2 months from production [38].

Figure 25a presents XRD tests used for the characterization of a traditional (reference) sample containing quartz sand (QS). The following phases and minerals were present in a traditional brick sample: tobermorite 9A,  $\text{SiO}_2$  ( $\alpha$ ), and calcium aluminum silicate. In a sample modified with glass sand (GS, Figure 25b), the following minerals were found to be present: gyrolite and natrolite, and as for the reference material, also tobermorite. Figure 26 is an XRD analysis (X-ray diffraction) of the reference autoclaved brick (upper half of the photo) and glass sand modified with 90% (GS-lower half of the photo) after 36 months from the production date. The samples were stored at temperatures between 23 and 28 °C throughout the period. Glass sand is characterized by an amorphous structure and is thermodynamically metastable (it reacts to changes in temperature and pressure). As the XRD test shows, we dealt with the crystallization of a modified material. Apart from the method of storing the tested material, the situation may also be influenced by the fact that the hydration temperature (in the presence of glass sand) during lime slaking was approximately 40 °C. XRD analysis provides information about the crystal structure and phase composition of the material. The disadvantage of this method is that it is difficult to determine the phases from complex diffraction patterns obtained from multiphase materials.

Two variants were considered in the studies, the first being where the C-S-H phase could precipitate, and the second where the formation of the C-S-H phase was inhibited in the calculations. In the first stimulation of the phases in which they were predicted to be present in the material, at 20 °C and 1 bar pressure, the following were identified: C-S-H, natrolite, gyrolite, and magnesium silicate hydrate (M-S-H), analogous to C-S-H and occurring in systems with increased magnesium content, for example, slag cements. At the second stimulation, where the C-S-H phase was suppressed, natrolite, gyrolite, and brucite were identified.

The GEMS-PSI program was used to analyze the phase state of the samples [69]. The GEMS program is important as it takes into account the base minerals and phases present in building materials, with particular emphasis on concrete and cement, which, in turn, are composed of the C-S-H phase, which corresponds to their durability and strength. Before undertaking thermodynamic simulations using the GEMS-PSI program, XRF analysis (Figure 27) was performed, which was necessary to determine and calculate the input oxide

compositions of the mixtures used to manufacture bricks. The first test that was performed was X-ray fluorescence spectroscopy, which is a technique that determines the qualitative and quantitative analysis of the elemental composition of the sample tested. Elemental composition analysis is an important starting point for the investigation. Thermodynamic properties (using the GEMS-PSI program) of materials modified by 90% GS and phases tested in this article are shown in Figure 28. This type of test determines the chemical and mechanical properties, as well as further microstructural properties in terms of the formation of amorphous and crystalline phases. Then, XRD tests were performed. In the case of the presented geochemical modeling analysis of the obtained data, various cases can be considered, e.g.:

- (a) Possible precipitation of the C-S-H phase.
- (b) No possibility of C-S-H phase precipitation (C-S-H is suppressed in the calculation).

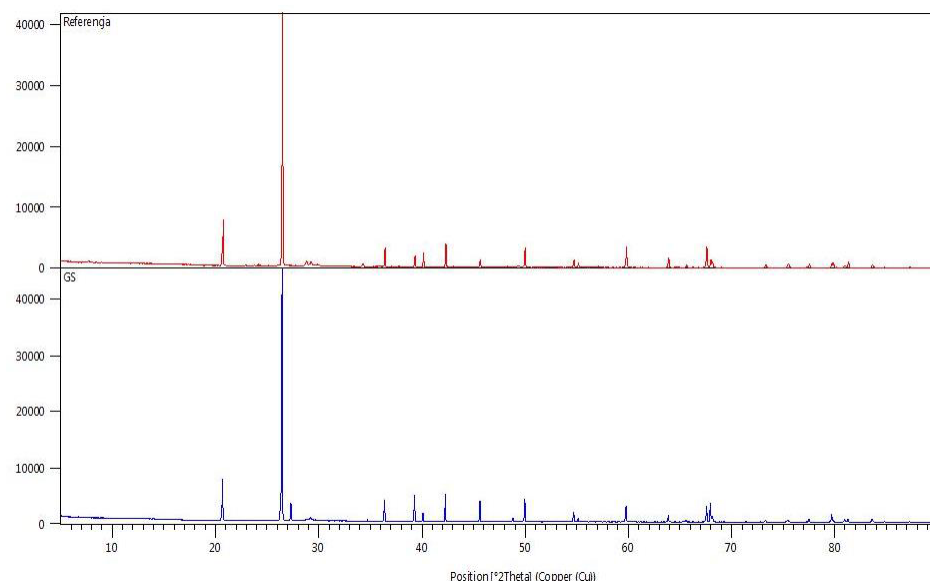


**Figure 26.** Samples (reference and modified by GS) after 36 months (crystallization).

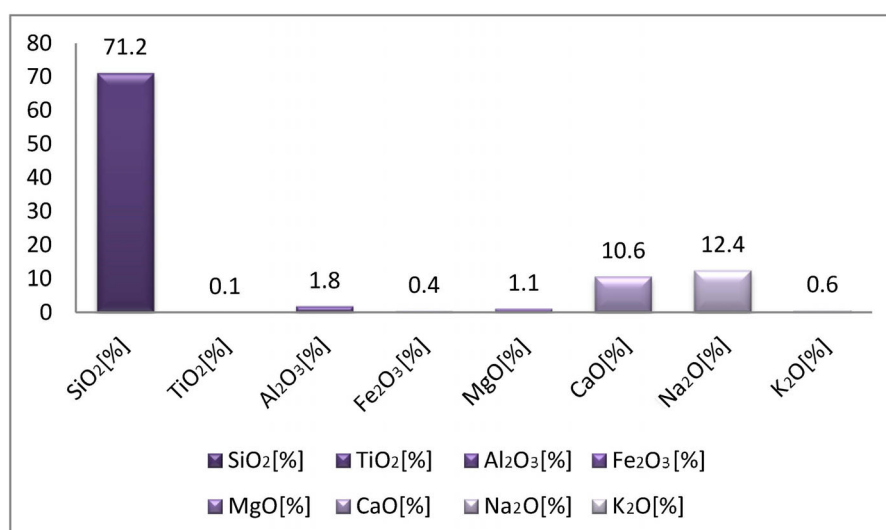


**Figure 27.** XRF (elemental composition) analysis (oxide composition) of silicate brick modified with glass sand [37].

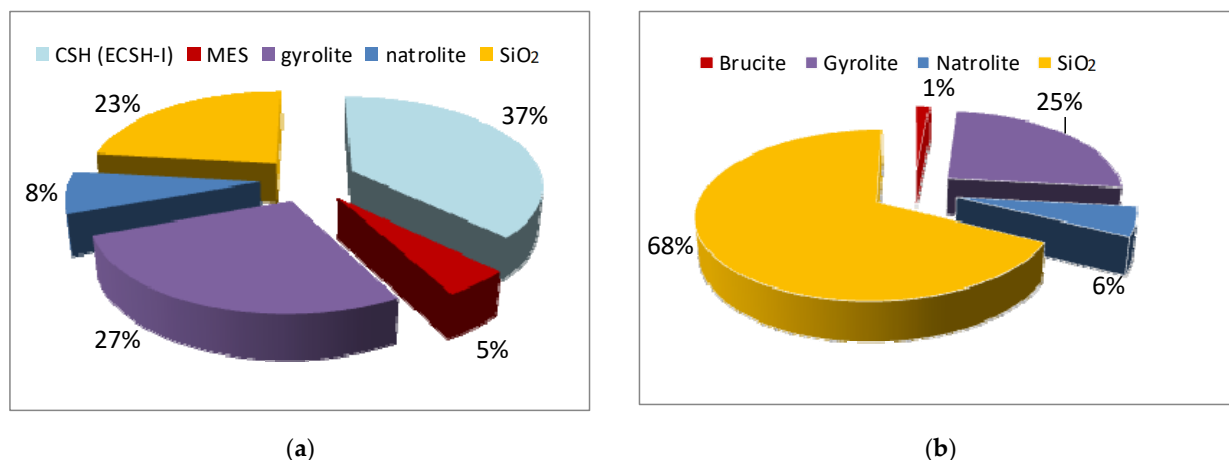


**Figure 28.** (a) Volume% of solids predicted by thermodynamic simulation at 25 °C, 1 bar. (b) Volume% of solids predicted by thermodynamic simulation at 25 °C, 1 bar. In this simulation, precipitation of C-S-H (ECSH-I) was suppressed.

Each time, it is necessary to know the production process of the analyzed material and the quality of the substrates used for its production.

The GEMS-PSI package [69], as part of thermodynamic modeling, was used to quantify the influence of the precursor, i.e., the type of binder (lime as the activating material), chemical composition, and the content of individual substrates for the tested materials (sand-lime bricks) on the phase assemblies, and thus attempts to determine the durability of modified materials (due to, among others, the process of crystallization of the C-S-H phase). Combined with experimental assessments of phase groupings (including the use of X-ray analysis) and porosity analysis, this information was used to identify potentially suitable combinations of the use of glass sand in silicate mass. The calculations also provide information on the “durability ratios” regarding the stability of individual phases and solid hydrates and the risk of harmful processes such as: temperature rise, sulfate (and thaumasite) attack, corrosion, and decalcification reactions to which the material is exposed during operation in the field [45].

Two research paths have been presented: one where the C-S-H phase was allowed to precipitate, and the second one where the C-S-H formation was suppressed in the calculation. The second research path, i.e., blocking the precipitation of the C-S-H phase, is more likely due to the technological process of brick production and the high temperature of autoclaving (200 °C). During both simulations, the phases were anticipated to be present in the material using a temperature of 25 °C and a pressure of 1 bar (1 atm). Figure 28 and Table 3 show the volume of the solid in laboratory autoclaved bricks modified by 90% glass sand (GS). Analysis of the microstructure with the GEMS-PSI package allowed for the determination of the quality and number of phases in the material modified by GS. The analysis showed the presence of the following phases (as a function of volume, Figure 28a): 37% by volume of the material is the C-S-H phase, the next 27% is gyrolite, 23% is sand, 8% is natrolite, and 5% is the M-S-H phase (due to the presence of magnesium compounds in the substrates for the production of silicate brick). Figure 28b shows the volume of the solid of a laboratory brick modified by 90% GS with an obstructed C-S-H phase and with ‘turning off’ the C-S-H phase during thermodynamic simulation. In this case, the following structures were created: 68% sand, 25% of gyrolite, 6% of natrolite, and 1% of brucite.

**Table 3.** Thermal dynamics (geochemical modeling, GEMS) simulation results obtained at 25 °C.

Type of Phase	Volume of Solid Phases [cm <sup>3</sup> ]	Volume of Solid Phases [cm <sup>3</sup> ] (Suppressed C-S-H Phase)
C-S-H (ECSH-I)	132.84	-
MSH (magnesium silicate hydrate)	17.11	-
Gyrolite	97.28	118.02
Natrolite	26.55	26.55
Brucite	-	6.72
SiO <sub>2</sub>	82.45	324.66

Without the knowledge of the sample and the GEMS-SPI program [69], it is only possible to theoretically predict the phases that make up the microstructure of the analyzed material, the manner of their precipitation, the amount, and thus the durability of the material. Modified brick materials change over time. Applied modifications may result in favorable characteristics (e.g., the shortening of autoclaving time while achieving the same or higher compressive strength values, density at the same level as the reference silicate brick, use of recycled waste glass and its utilization in building materials such as autoclaved bricks), but does not necessarily mean durability of the material over time. Thus, GEMS-PSI geochemical modeling (Gibbs energy minimization software for geochemical modeling) allows for the prediction of the method of crystallization of the materials, their behavior under the influence of environmental changes, thermodynamic conditions, and analysis of the possibility of CO<sub>2</sub> absorption by the material, which has a positive impact on environmental protection and is included in a sustainable economy and sustainable construction.

The standard molar thermodynamic properties of minerals formed in tested bricks (traditional: C-S-H, tobermorite, grossular, xonotlite, and SiO<sub>2</sub>) and material modified by 90% GS (C-S-H, gyrolite, natrolite) are presented below (Table 4).

**Table 4.** Standard molar thermodynamic properties of minerals found in tested bricks [37,38,79].

Mineral Name	Formula	Δ <sub>f</sub> G° [kJ/mol]	Δ <sub>f</sub> H° [kJ/mol]	S° [J/K·mol]	C° <sub>p</sub> [J/K·mol]	V° [cm <sup>3</sup> /mol]	M [g/mol]
C-S-H	Ca <sub>0.8</sub> SiO <sub>2.8</sub> :1.54H <sub>2</sub> O	-1769.0	-1945.13	107.850	138.3	59.2	132.6
Tobermorite 11A	Ca <sub>5</sub> Si <sub>6</sub> O <sub>16</sub> (OH) <sub>2</sub>	-9889.3	-10,680.0	692.5	764.9	286.1	739.9
Grossular	Ca <sub>3</sub> Al <sub>2</sub> Si <sub>3</sub> O <sub>12</sub>	-6279.6	-6640.	260.1	327.8	125.3	450.4
α-SiO <sub>2</sub>		-856.2	-910.7	41.4	44.5	22.6	60.0
β-SiO <sub>2</sub>		-854.9	-908.6	43.7	44.7	-	60.0
Gyrolite	Ca <sub>2</sub> Si <sub>3</sub> O <sub>7.5</sub> (OH)·2H <sub>2</sub> O	-4550	-4917	309	325	137	337.4
Natrolite	Na <sub>2</sub> (Al <sub>2</sub> Si <sub>3</sub> )O <sub>10</sub> :2H <sub>2</sub> O	-5316.6	-5718.6	359	359.2	169.2	380.2
Brucite	Mg(OH) <sub>2</sub>	-831.99	-924.1	59.4	77.3	24.6	58.3
Xonotlite	Ca <sub>6</sub> Si <sub>6</sub> O <sub>17</sub> (OH) <sub>2</sub>	-9465	-10,022	573	628	256.9	714.9

Δ<sub>f</sub>G°—standard molar Gibbs free energy of formation at T<sub>o</sub> = 298 K; Δ<sub>f</sub>H°—standard molar enthalpy at T<sub>o</sub> = 298 K; S°—standard molar entropy at T<sub>o</sub> = 298 K; C°<sub>p</sub>—heat capacity at T<sub>o</sub> = 298 K; V°—molar volume; and M—molar mass.

#### 4. Discussion

Every building material can be modified with every possible, accessible, and safe material, but it is necessary to test the durability of the modified materials not only after 28 or 90 days from their production, but also after a longer period of time in order to determine the level of early and long-term strength. The presented analyses, tests, and studies were conducted in the years 2016–2022. Most discussions and doubts were caused by the inefficiency of modifications in terms of inadequate and time-consuming research and analysis, as well as phase changes in the structure (material microstructure), which

are responsible for the functional properties of building materials (including silicate brick). Silicate brick is a material resistant to environmental conditions, as it is created under high pressure and temperature, which ensures its durability. It is necessary to establish chemical reactions, phase changes (change in the specific surface due to crystallization of amorphous phases), and mechanical properties in terms of material durability. Moreover, many materials (including glass) have a tendency to swell when the raw material components are not properly selected (including incorrect assumptions and parameters, e.g., incorrect, too large, too small grain diameter, or inappropriate selection of the fraction). Questions about stability can be answered by using thermodynamic modeling approaches, which, based on the XRF analysis input parameters, can make it possible to estimate the quantity and quality of amorphous and crystalline phases in the sample of the tested material. As the XRD test shows, we dealt with the crystallization of a modified material. Apart from the method of storing the tested material, the situation may also be influenced by the fact that the hydration temperature (in the presence of glass sand) during lime slaking was only approximately 40 °C. Glass sand, as a metastable and amorphous material, retains properties similar to fly ash and undergoes crystallization. After the analysis of the elemental composition and the production temperature (autoclaving of silicate brick), it was possible to make a phase selection, i.e., to mark which of the phases has the possibility of synthesis and crystallization, and which will not be formed or will be in deficit. As shown by research using the GEMS-PSI package, it is possible to crystallize the C-S-H phase in the direction of: M-S-H, gyrolite, and natrolite. Additionally, after ‘quenching’ the C-S-H phase, crystallization takes place in the direction of: brucite, gyrolite, and natrolite. The use of the geochemical modeling code made it possible to examine the potential direction of crystallization and determine the effectiveness of the modification, which, combined with the functional properties (compressive strength, density, and porosity), provided good results, also limiting energy losses during unfavorable experiments, including those that may endanger the environment. Depending on the introduced conditions (pressure, temperature, and CO<sub>2</sub> concentration), these phases may also change, therefore, further observations of the indicated materials (modified glass sand) are important. However, the presented modification is a beneficial solution, especially for secondary construction (small outbuildings, rooms, and temporary construction), e.g., in times of crisis (conflicts, natural disasters), when people lose their homes, or it is necessary to build buildings that serve as shelter. This kind of modification does not require changes in the production process (Figure 29) or on the production line. The only substrate to be replaced or supplemented (depending on the intended use of the material and expectations towards glass sand bricks) is the addition of glass sand (GS) together with, or as a substitute for, quartz sand (QS).

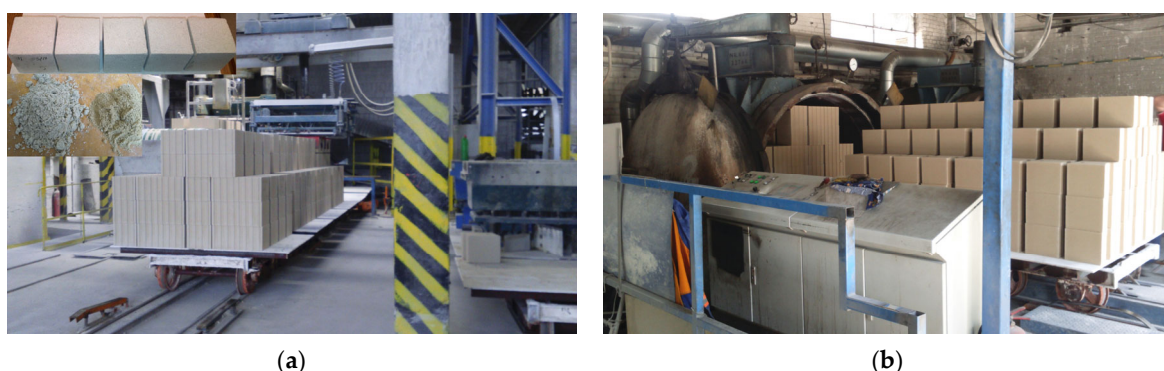


**Figure 29.** Example silicate brick production line (Ludynia, Poland); (a) pressing process under pressure of fresh silicate mass; (b) autoclaving process of pressed and formed silicate brick under pressure.

Subsequently, porosity tests will be performed using the Archimedes method, GEMS simulations in various temperature ranges (25–200 °C) after 7 years from the date of production of bricks based on glass sand and bricks with the use of various types of glass,

and a comparison of the microstructural properties of the analyzed materials. Hardness tests of materials based on glass sand will also be performed.

## 5. Conclusions

The studies presented in this paper show the effect of the addition of recycled amorphous glass sand (GS) on the individual properties of these types of products. Research on modified materials should be repeated and analyzed as a function of time. Autoclaved materials differ from concrete, primarily in their method of production, which causes the difference in their structure and microstructure. In concrete, the dominant phase is the amorphous C-S-H phase, and the deficit phases are those with a crystalline structure. The opposite situation is observed in the case of autoclaved materials, especially silicate bricks. In this type of brick, the deficit phase is the C-S-H phase, which is a metastable phase, i.e., it is thermodynamically stable up to 30 °C, then, depending on the given conditions (temperature, pressure) or composition (components, binder), crystallization occurs towards jennite (in the case of high quantity of binder) or tobermorite (poor materials in binder, e.g., silicate bricks, which consist of 7% of CaO). Crystallization can also take place in the direction of natrolite or gyrolite in the case of glass components (as indicated by the addition of sodium oxides from bottle glass). The presented tests were selected 36 months after the samples were created. SEM photos were also taken after 6 years from the date of production of the laboratory bricks in order to visually verify the modified microstructure. The compressive strength of the traditional silicate material is approximately 15–20 MPa. In laboratory conditions, when increasing the share of GS, higher values of compressive strength were obtained (up to the optimal level of 20.3 MPa in relation to the traditional laboratory brick—the structure of the modified material has been compacted). The user-relevant total utility analysis confirms that the optimum glass sand content is 60% with 4% water, giving a compressive strength value of over 15 MPa (15.729 MPa) with a utility of approximately 0.71.

The main aspect of the research was the study of microstructure in the context of mechanical properties. The microstructure of the material changed, as a small amount of material modified with glass sand (90% GS) crystallized. Analysis of the microstructure with the GEMS-PSI package allowed for the determination of the quality and number of phases in the material modified by GS. The analysis showed the presence of the following phases: 37% by volume of the material is the C-S-H phase, 27% gyrolite, 23% sand, 8% natrolite, and 5% the M-S-H phase. The next test showed that the volume of solid for the laboratory brick was modified by 90% GS when the C-S-H phase formation was suppressed during the thermodynamic simulation. In that case, the following structures were created: 68% sand, 25% gyrolite, 6% natrolite, and 1% brucite. The quality of modified materials depends on their internal structure; therefore, the tests should be continued and extended with further tests. Looking at the elemental composition, it can be concluded that the presence of Fe<sub>2</sub>O<sub>3</sub> in the glass components positively affects the strength properties of the modified silicate brick. Similarly, the results of Abdoliyazdi and all [80] proved that the mechanical properties of samples with the addition of 1 and 3% of Fe<sub>2</sub>O<sub>3</sub> nanoparticles are beneficial. The study of the microstructure of cement mortars containing ordinary and Fe<sub>2</sub>O<sub>3</sub> nanoparticles showed that Fe<sub>2</sub>O<sub>3</sub> nanoparticles fill pores and reduce large Ca(OH)<sub>2</sub> crystals, and hydrate products. Moreover, they are denser and more compact. The thesis above was also confirmed by the modification of the silicate mass with glass sand (there was an increase in strength values, an improvement in density (more specifically, an increase in the number of micropores) as a result of structure compaction, and a decrease in water absorption, although this is also related to the humidity of the glass sand added to the raw material mass). Research on autoclaved sand-lime bricks modified by glass sand will be continued. According to strength analysis, brick samples with a content of 60% GS, 30% QS, 4% H<sub>2</sub>O, and 6–7% CaO will be created again. The research will particularly apply to microstructural changes in bricks with GS due to the impact of atmospheric conditions (e.g., on the formation of crevices, pores, and phase crystallization). However, the tests

suggest that this type of modified brick can be used in construction. First of all, this can be material for buildings, and temporary buildings, which will contribute to relieving natural deposits and helping reduce the growing deficit of quartz aggregate.

**Funding:** The conducted research and analyses are the result of a scientific internship at the University of Sherbrooke (2015/2016-sabbatical leave), academic internship at the University of California, Los Angeles (2019—Miniature 2 Grant No.: 2018/02/X/ST8/00544 and 2022 RID: “The project is supported by the program of the Minister of Science and Higher Education under the name: “Regional Initiative of Excellence” in 2019–2022 project number 025/RID/2018/19 financing amount PLN 12,000,000”).

**Acknowledgments:** The author would like to acknowledge to every person who strengthened my position as a scientist, gave substantive tips and opportunities for international internships, namely professors from the University of California Los Angeles, Civil Engineering and Environmental Department, Institute for Carbon Management (LA, USA), University of Sherbrooke, Department of Civil Engineering (Quebec, Canada), AGH University in Cracow (Poland) and the current academic authorities from KUT in Kielce (Poland).

**Conflicts of Interest:** The authors declare no conflict of interest.

### Nomenclatures

QS	Quartz Sand
GS	Glass Sand
GP	Glass Powder
XRF	X-ray Powder Diffraction
SEM	Scanning Electron Microscope
XRD	X-ray Powder Diffraction [keV]
CT	computed tomography used for building materials to visualize the porous structure (non-destructive testing)
GEMS-PSI	Gibbs Energy Minimization Software for Geochemical Modeling—Paul Scherrer Institut
V	molar volume [ $\text{cm}^3 \cdot \text{mol}^{-1}$ ]
M	molar mass [ $\text{g} \cdot \text{mol}^{-1}$ ]
T	Temperature [ $^\circ\text{C}$ or K]
Log10K	solubility product at T= 298 K ( $25^\circ\text{C}$ )(this information is the basis for determining the pH of the material)
$\Delta fG^\circ$	standard Gibbs free energy of formation [ $\text{J} \cdot \text{mol}^{-1}$ ]
$\Delta fH^\circ$	standard enthalpy of formation, is the change in enthalpy when one mole of a substance is formed from its elements under a standard pressure of 1 atm/1 bar [ $\text{J} \cdot \text{mol}^{-1}$ ]
$C_p^\circ$	specific heat [ $\text{J} \cdot \text{mol}^{-1} \cdot \text{K}^{-1}$ ]
$S^\circ$	standard entropy of formation [ $\text{J} \cdot \text{mol}^{-1} \cdot \text{K}^{-1}$ ]
C-S-H	Calcium Silicate Hydrate
M-S-H	Magnesium Silicate Hydrate

### References

- Guven, G.; Arceo, A.; Bennett, A.; Tham, M.; Olanrewaju, B.; McGrail, M.; Isin, K.; Olson, A.W.; Saxe, S. A construction classification system database for understanding resource use in building construction. *Sci. Data* **2022**, *9*, 42. Available online: <https://www.nature.com/articles/s41597-022-01141-8> (accessed on 26 February 2023). [CrossRef] [PubMed]
- Stepien, A.; Dachowski, R.; Piotrowski, J.Z. Insulated Autoclaved Cellular Concretes and Improvement of Their Mechanical and Hydrothermal Properties. In *Thermal Insulation and Radiation Control Technologies for Buildings*; Kosny, J., Yarbrough, D.W., Eds.; Springer: Cham, Switzerland, 2022; pp. 393–419. ISBN 978-3-030-98693-3. Available online: <https://link.springer.com/book/10.1007/978-3-030-98693-3> (accessed on 5 February 2023).
- Kozioł, W.; Baic, I. Kruszywa naturalne w Polsce—Aktualny stan i przyszłość/Natural aggregates in Poland—Current state and future. *Przegląd Górnictwy* **2018**, *74*, 1–8.
- Kozioł, W.; Machniak, Ł.; Borcz, A.; Baic, I. Mining of aggregates in Poland—Opportunities and threats. *Inżynieria Miner. J. Pol. Miner. Eng. Soc.* **2016**, *2*, 175–182.
- Available online: <https://www.conserve-energy-future.com/sustainable-construction-materials.php> (accessed on 12 January 2023).

6. Apak, K. Traditional Wall Construction Technology of the Ottoman Empire in Relation to the Seismic Resistance of Bath Structures in the Marmara Region. In *Structural Analysis of Historical Constructions*; Aguilar, R., Torrealva, D., Moreira, S., Pando, M.A., Ramos, L.F., Eds.; Springer: Cham, Switzerland, 2023; Volume 18, pp. 250–258.
7. Available online: <https://budownictwob2b.pl/przegrody/baza-wiedzy/sciany-i-stropy/21054-grupa-silikaty-jakie-parametry-scian-sa-najwazniejsze> (accessed on 12 January 2023).
8. Available online: <https://jw-a.pl/2019/06/co-to-jest-zrownowazone-budownictwo/> (accessed on 12 January 2023).
9. PN-EN ISO 14040:2009/A1:2021-03; Zarządzanie Środowiskowe—Ocena Cyklu Życia—Zasady i Struktura/Environmental Management—Life Cycle Assessment—Principles and Structure. Polish Standardization Committee PKN: Warsow, Poland, 2021. Available online: <https://sklep.pkn.pl/pn-en-iso-14040-2009-a1-2021-03e.html> (accessed on 13 February 2023).
10. PN-EN ISO 14044:2009/A1:2018-05; Zarządzanie Środowiskowe—Ocena Cyklu Życia—Wymagania i Wytyczne/Environmental Management—Life Cycle Assessment—Requirements and Guidelines. Polish Standardization Committee PKN: Warsow, Poland, 2018. Available online: <https://sklep.pkn.pl/pn-en-iso-14044-2009-a1-2018-05e.html> (accessed on 17 January 2023).
11. PKN-ISO/TR 14047:2006; Zarządzanie Środowiskowe—Ocena Wpływów Cyklu Życia—Przykłady Stosowania/Environmental Management—Life Cycle Impact Assessment—Application Examples. Polish Standardization Committee PKN: Warsow, Poland, 2006. Available online: <https://sklep.pkn.pl/pkn-iso-tr-14047-2006p.html> (accessed on 13 February 2023).
12. Available online: <https://eur-lex.europa.eu/legal-content/EN/TXT/?uri=celex%3A32011R0305> (accessed on 19 January 2023).
13. Available online: <https://blog.synthesia.com/pl/czym-jest-budownictwo-zrownowazone-troce-historii> (accessed on 1 February 2023).
14. Available online: <https://climate.nasa.gov/news/2915/the-atmosphere-getting-a-handle-on-carbon-dioxide/#:~:text=The%20concentration%20of%20carbon%20dioxide,it%20was%20near%20370%20ppm> (accessed on 23 January 2023).
15. Available online: <https://sdgs.un.org/goals> (accessed on 2 February 2023).
16. Pawłowski, K. Warunki Techniczne 2021 dla Przegród i Złączów Budowlanych/Technical Conditions 2021 for Building Partitions and joints. Thermal Quality of Building Partitions and Joints in Buildings Taking into Account the Requirements in Force since 1 January 2021. IZOLACJE 11/12/2020, 16 December 2020. Available online: <https://www.izolacje.com.pl/artykul/termomodernizacja/247229,warunki-techniczne-2021-dla-przegrod-i-zlaczki-budowlanych> (accessed on 11 February 2023).
17. Musiał, M.; Licholai, L.; Pękala, A. Analysis of the Thermal Performance of Isothermal Composite Heat Accumulators Containing Organic Phase-Change Material. *Energies* **2023**, *16*, 1409. [[CrossRef](#)]
18. Martin, G. New Stanford Research Reveals the Secrets of Stishovites, a Rare Form of Crystallized Sand. *Stanford Engineering* **8 December 2015**. Available online: <https://engineering.stanford.edu/magazine/article/new-stanford-research-reveals-secrets-stishovites-rare-form-crystallized-sand> (accessed on 9 March 2023).
19. Available online: [https://www.nature.com/scitable/blog/saltwater-science/what\\_is\\_sand\\_made\\_of](https://www.nature.com/scitable/blog/saltwater-science/what_is_sand_made_of) (accessed on 12 January 2023).
20. Available online: <https://geology.com/> (accessed on 11 January 2023).
21. Ziegler, V. Factors Influencing the Rounding of Sand Grains. *J. Geol.* **1911**, *19*, 645–654. Available online: <https://www.jstor.org/stable/30061452> (accessed on 4 February 2023). [[CrossRef](#)]
22. Available online: <https://www.bbc.com/future/article/20191108-why-the-world-is-running-out-of-sand> (accessed on 5 February 2023).
23. Available online: <https://innpoland.pl/169047,koncza-sie-globalne-zasoby-piasku-pod-inwestycje-i-szaleja-mafie-piaskowe> (accessed on 3 February 2023).
24. Gao, J.; Zhong, X.; Cai, W.G.; Ren, H.; Huo, T.; Wang, X.; Mi, Z. Dilution effect of the building area on energy intensity in urban residential buildings. *Nat. Commun.* **2019**, *10*, 4944. [[CrossRef](#)]
25. Available online: <https://zielona.interia.pl/przyroda/news-na-swicie-konczy-sie-piasek-budowlany-a-popyt-na-niego-gwał,nId,5922863> (accessed on 3 January 2023).
26. Shilpa, R.; Kumar, P.R. Effect of Using Glass Powder in Concrete. In Proceedings of the International Conference on Innovations & Advances in Science, Engineering and Technology, IC-IASET 2014, Kerala, India, 16–18 July 2014.
27. Oey, T.; Timmons, J.; Stutzman, P.; Bullard, W.J.; Balonis, M.; Mauchy, M.; Sant, G. An improved basis for characterizing suitability of fly ash as a cement replacement agent. *J. Am. Ceram. Soc.* **2017**, *100*, 4785–4800. [[CrossRef](#)]
28. Khomchenko, Y.V.; Semeykin, A.Y. Improving the Efficiency and Safety in the Technology of Lime and Silicate Materials. *Mater. Sci. Forum* **2019**, *974*, 243–248. [[CrossRef](#)]
29. Soliman, N.A.; Taguit-Hamou, A. Development of ultra-high-performance concrete using glass powder—Towards ecofriendly concrete. *Constr. Build. Mater.* **2016**, *125*, 600–612. [[CrossRef](#)]
30. Taha, B.; Nounou, G. Utilizing Waste Recycled Glass as Sand/Cement Replacement in Concrete. *J. Mater. Civ. Eng.* **2009**, *21*, 709–721. [[CrossRef](#)]
31. Taylor, H.F.W. *Cement Chemistry*; Thomas Telford Publishing: London, UK, 1997.
32. Hong, S.Y.; Glasser, F.P. Phase relations in the CaO–SiO<sub>2</sub>–H<sub>2</sub>O system to 200 °C at saturated steam pressure. *Cem. Concr. Res.* **2004**, *34*, 1529–1534. [[CrossRef](#)]
33. Maschio, S.; Tonello, G.; Furlani, E. Recycling Glass Cullet from Waste CRTs for the Production of High Strength Mortars. *J. Waste Manag.* **2013**, *2013*, 102519. [[CrossRef](#)]
34. Orouji, M.; Najaf, E. Effect of GFRP rebars and polypropylene fibers on flexural strength in high-performance concrete beams with glass powder and microsilica. *Case Stud. Constr. Mater.* **2023**, *18*, e01769. [[CrossRef](#)]

35. Afshinnia, K. Waste Glass in Concrete has Advantages and Disadvantages. *Concr. Décor Technol. Concr. Placing* **2019**, *19*. Available online: <https://www.concretedecor.net/departments/concrete-placing/waste-glass-in-concrete-has-advantages-and-disadvantages/> (accessed on 9 March 2023).
36. Stepień, A. Analysis of Porous Structure in Autoclaved Materials Modified by Glass Sand. *Crystals* **2021**, *11*, 408. [CrossRef]
37. Stepień, A.; Potrzeszcz-Sut, B.; Prentice, D.P.; Oey, T.; Balonis, M. The Role of Glass Compounds in Autoclaved Bricks. *Buildings* **2020**, *10*, 41. [CrossRef]
38. Stepień, A.; Leśniak, M.; Sitarz, M. A Sustainable Autoclaved Material Made of Glass Sand. *Buildings* **2019**, *9*, 232. [CrossRef]
39. Stepień, A.; Kostrzewa, P. The impact of glass components on the quality and strength of silicate autoclaved materials. *IOP Mater. Sci. Eng.* **2019**, *471*, 032064. [CrossRef]
40. Stepień, A. The Impact of Glass Additives on the Functional and Microstructural Properties of Sand-Lime. *Int. J. Civil Environ. Eng.* **2017**, *11*, 1–8.
41. Exploring The Amorphous, Siliceous Solid That Is Glass, 13 November 2021. Available online: <https://www.scienceandpandas.com/exploring-the-amorphous-siliceous-solid-that-is-glass/> (accessed on 9 March 2023).
42. Available online: <https://www.e-education.psu.edu/mats81/node/2154> (accessed on 9 March 2023).
43. Yang, Y.; Zhou, J.; Zhu, F.; Yuan, Y.; Chang, D.J.; Kim, D.S.; Pham, M.; Rana, A.; Tian, X.; Yao, Y.; et al. Determining the three-dimensional atomic structure of an amorphous solid. *Nature* **2021**, *592*, 60–64. [CrossRef]
44. Tamanna, N.; Tuladhar, R.; Sivakugan, N. Performance of recycled waste glass sand as partial replacement of sand in concrete. *Constr. Build. Mater.* **2020**, *239*, 117804. [CrossRef]
45. Małek, M.; Łasica, W.; Jackowski, M.; Kadela, M. Effect of Waste Glass Addition as a Replacement for Fine Aggregate on Properties of Mortar. *Materials* **2020**, *13*, 3189. [CrossRef] [PubMed]
46. Reaktywność Alkaliczna Kruszyw/Alkaline Reactivity of Aggregates/Alkaline Reactivity of Aggregates. Available online: [https://www.gorazdze.pl/pl/system/files\\_force/assets/document/a7\\_reaktywnosc\\_alkaliczna\\_kruszyw.pdf?download=1](https://www.gorazdze.pl/pl/system/files_force/assets/document/a7_reaktywnosc_alkaliczna_kruszyw.pdf?download=1) (accessed on 6 April 2023).
47. Taha, B.; Nounou, G. Properties of Concrete Contains Mixed Colour Waste Recycled Glass as Sand and Cement Replacement. *Constr. Build. Mater.* **2008**, *22*, 713–720. [CrossRef]
48. Taghit-Hamou, A.; Bengougam, A. Glass Powder as a Supplementary Cementitious Material. *Concr. Int.* **2012**, *34*, 56–61.
49. Xiao, R.; Huang, B.; Zhou, H.; Ma, Y.; Jiang, Y. A state-of-the-art review of crushed urban waste glass used in OPC and AAMs (geopolymer): Progress and challenges. *Clean. Mater.* **2022**, *4*, 100083. [CrossRef]
50. Jiang, X.; Xiao, R.; Bai, Y.; Huang, B.; Ma, Y. Influence of waste glass powder as a supplementary cementitious material (SCM) on physical and mechanical properties of cement paste under high temperatures. *J. Clean. Prod.* **2022**, *340*, 130778. [CrossRef]
51. Sobolev, K.; Türker, P.; Soboleva, S.; Iscioglu, G. Utilization of waste glass in ECO-cement: Strength properties and microstructural observations. *Waste Manag.* **2007**, *27*, 971–976. [CrossRef]
52. Siauciunas, R.; Baltakys, K. Formation of gyrolite during hydrothermal synthesis in the mixtures of CaO and amorphous SiO<sub>2</sub> or quartz. *Cem. Concr. Res.* **2004**, *34*, 2029–2036. [CrossRef]
53. Richardson, I. Tobermorite/jennite- and tobermorite/calcium hydroxide-based models for the structure of C-S-H: Applicability to hardened pastes of tricalcium silicate, beta-dicalcium silicate, Portland cement, and blends of Portland cement with blast-fumace slag, metakaolin, or silica fume. *Cem. Concr. Res.* **2004**, *34*, 1733–1777.
54. Kittipong, K.; Suwimol, A.; Kwannate, S. *Effect of Fine Al-Containing Waste in Autoclaved-Aerated; Concrete Incorporating Rice-Husk Ash 10.1061/(ASCE), MT.1943-5533.0001149*; American Society of Civil Engineers: Reston, VA, USA, 2014.
55. Baltušnikas, A.; Lukošiūtė, I.; Baltakys, K. XRD Characterization of Organically Modified Gyrolite. *Mater. Sci. (Medžiagotyra)* **2009**, *15*, 325.
56. Barišić, I.; Zvonarić, M.; Netinger Grubeša, I.; Šurdonja, S. Recycling waste rubber tyres in road construction. In *Archives of Civil Engineering*; Polish Academy of Sciences: Warsaw, Poland, 2021; Volume LXVII.
57. Mohajerani, A.; Burnett, L.; Smith, J.V.; Markovski, S.; Rodwell, G.; Tareq Rahman, M.D.; Kurmus, H.; Mirzababaei, M.; Arulrajah, A.; Horpibulsuk, S.; et al. Recycling waste rubber tyres in construction materials and associated environmental considerations: A review. *Resour. Conserv. Recycl.* **2020**, *155*, 104679. [CrossRef]
58. Hu, Y.; Sun, X.; Ma, A.; Gao, P. An Experimental Study on the Basic Mechanical Properties and Compression Size Effect of Rubber Concrete with Different Substitution Rates. *Adv. Civ. Eng.* **2020**, *2020*, 8851187. [CrossRef]
59. Zheng, W.; Sheng, X.; He, H.; Xu, H.; Yang, Y. Use of Rubber Mat to Improve Deformation Behaviors of Ballastless Tracks Laid on Bridges. *Adv. Civ. Eng.* **2020**, *2020*, 8821402. [CrossRef]
60. PN-EN 772-13; Methods of Test for Masonry Units-Part 13: Determination of the Density of the Net and Gross Density of Masonry in the Dry State (Except for Natural Stone). CEN: Brussels, Belgium, 2001.
61. PN-EN 1996-2; Eurocode 6-Design of Masonry Structures-Part 2: Design, Selection of Materials and Execution of Masonry. CEN: Brussels, Belgium, 2010.
62. PN-EN 771-2; Specification for Masonry Units. Part 2: Calcium Silicate Masonry Units. CEN: Brussels, Belgium, 2010.
63. PN-EN 772-1; Standard Replaced by PN-EN 772-1+A1:2015-10: Test Methods for Masonry Units—Part 1: Determination of Compressive Strength. The European Standard Establishes a Method for Determining the Compressive Strength of Masonry Units. Polish Standardization Committee: Warsaw, Poland, 2015.

64. PN-EN 1936; 2010—Natural Stone Test Methods—Determination of Density and Bulk Density as Well as Total and Open Porosity. CEN: Brussels, Belgium, 2010.
65. PN-EN 993-1; 2019-01—Test Methods for Compact Molded Refractory Products—Part 1: Determination of Apparent Density, Open Porosity and Total Porosity. CEN: Brussels, Belgium, 2019.
66. *Statistica 10.0—Advanced Data Analysis Software Suite, Originally Developed by StatSoft Inc./Pakiet Oprogramowania do Zaawansowanej Analizy Danych, Oryginalnie Opracowany Przez*; StatSoft Inc.: Tulsa, OK, USA, 2010.
67. Nermend, K. *Metody Analizy Wielokryterialnej i Wielowymiarowej We Wspomaganiu Decyzji*; Wydawnictwo Naukowe PWN: Warsaw, Poland, 2020.
68. Szafranko, E. Applicability of multi-criteria analysis methods for the choice of material and technology solutions in building structures. *Teh. Vjesn.* **2017**, *24*, 1935–1940.
69. Available online: <https://gems.web.psi.ch/> (accessed on 8 September 2022).
70. Osiecka, E. *Materiały Budowlane. Kamień. Ceramika. Szkło*; Oficyna Wydawnicza Politechniki Warszawskiej: Warsaw, Poland, 2003.
71. Klindt, L.B.; Klein, W. *Szkło Jak Materiał Budowlany/Glass as a Building Material*; Arkady: Warsaw, Poland, 1982.
72. Stepien, A. The Impact of Barium Sulfate on the Microstructural and Mechanical Properties of Autoclaved Silicate Products. In Proceedings of the 9th International Conference “ENVIRONMENTAL ENGINEERING”, Vilnius, Lithuania, 22–23 May 2014. [CrossRef]
73. Stepien, A. The influence of basalt aggregate on the porosity and the durability of silicate products. In *Issues Material in Construction and Environmental Engineering*; Iwański, M., Ed.; Kielce University of Technology: Kielce, Poland, 2012; pp. 37–46.
74. Stepien, A. Microstructural and functional properties of silicate products modified with basalt aggregate. In *Structure and Environment 1*; Kielce University of Technology: Kielce, Poland, 2012.
75. Stepien, A.; Dachowski, R. The impact of barium aggregate on the microstructure of sand-lime products. *Adv. Mater. Res.* **2011**, *250–253*, 618–621. Available online: <http://www.gbv.de/dms/tib-ub-hannover/664111637.pdf> (accessed on 4 February 2023).
76. Dachowski, R.; Stepien, A. The impact of various additives on the microstructure of silicate products. *Procedia Eng.* **2011**, *21*, 1173–1178. Available online: [www.sciencedirect.com/science/article/pii/S187705811049617](http://www.sciencedirect.com/science/article/pii/S187705811049617) (accessed on 4 February 2023). [CrossRef]
77. Hustavova, J.; Sebestova, P.; Meszarosova, L.; Cerny, V.; Drochytka, R. Usability of waste perlite in the technology of production of autoclaved aerated concrete. *IOP Conf. Ser. Mater. Sci. Eng.* **2019**, *549*, 012027. [CrossRef]
78. Stepien, A.; Durlej, M.; Skowera, K. Application of the computed tomography method for the evaluation of porosity of autoclaved materials. *Materials* **2022**, *15*, 8472. [CrossRef]
79. Available online: <http://thermoddem.brgm.fr/> (accessed on 11 May 2022).
80. Abdoliyazdi, N.; Arefi, M.R.; Mollaahmadi, E.; Abdollahi, B. To study the effect of adding Fe<sub>2</sub>O<sub>3</sub> nanoparticle on the morphology properties and microstructure of cement mortar. *Life Sci. J.* **2011**, *8*, 550–554.

**Disclaimer/Publisher’s Note:** The statements, opinions and data contained in all publications are solely those of the individual author(s) and contributor(s) and not of MDPI and/or the editor(s). MDPI and/or the editor(s) disclaim responsibility for any injury to people or property resulting from any ideas, methods, instructions or products referred to in the content.